Project No: 603502

DACCIWA

"Dynamics-aerosol-chemistry-cloud interactions in West Africa"

Deliverable

D4.3 Aerosol and cloud data

Due date of deliverable:	31/05/2017
Completion date of deliverable:	05/06/2017
Start date of DACCIWA project:	1st December 2013 **Project duration:** 60 months
Version:	[V1.0]
File name:	[D4.3_Aerosol_and_cloud_data_DACCIWA_v1.0.pdf]
Work Package Number:	**4**
Task Number:	**3**
Responsible partner for deliverable:	**UCA (former UPB)**
Contributing partners:	**UNIVMAN, DLR, CNRS**
Project coordinator name:	Prof. Dr. Peter Knippertz
Project coordinator organisation name:	Karlsruher Institut für Technologie

The DACCIWA Project is funded by the European Union's Seventh Framework Programme for research, technological development and demonstration under grant agreement no 603502.

Dissemination level		
PU	Public	**x**
PP	Restricted to other programme participants (including the Commission Services)	
RE	Restricted to a group specified by the consortium (including the Commission Services)	
CO	Confidential, only for members of the consortium (including the Commission Services)	

Nature of Deliverable		
R	Report	
P	Prototype	
D	Demonstrator	
O	Other	**x**

DOCUMENT INFO

Authors

Author	Beneficiary Short Name	E-Mail
Joel Brito, Régis Dupuy, Alfons Schwarzenboeck	UCA	J.Brito@opgc.univ-bpclermont.fr R.Dupuy@opgc.univ-bpclermont.fr A.Schwarzenboeck@opgc.univ-bpclermont.fr
Cyrielle Denjean, Thierry Bourrianne, Bruno Piguet	CNRM / MF	cyrielle.denjean@meteo.fr Thierry.bourrianne@meteo.fr Bruno.Piguet@meteo.fr cyrille.flamant@latmos.ipsl.fr
Christiane Voigt, Daniel Sauer, Anneke Batenburg	DLR	Christiane.Voigt@dlr.de; Daniel.Sauer@dlr.de
Hugh Coe, Jonathan Taylor	Univ Manchester	hugh.coe@manchester.ac.uk, jonathan.Taylor@manchester.ac.uk

Changes with respect to the DoW

Issue	Comments

Dissemination and uptake

Target group addressed	Project internal / external

Document Control

Document version #	Date	Changes Made/Comments
0.1	25.03.2017	Template with general structure
0.2	24.05.2017	Version for approval by the General Assembly
1.0	05.06.2017	Version approved by the General Assembly

Table of Contents

1 Executive summary

Deliverable D4.3 describes the aerosol-cloud interaction related datasets from 3 research aircraft that had been collected during field campaign which took place in 2016 between 25th June and 17th July. The three aircraft participating in the intensive aircraft campaign gathered high quality data, for WP 4 research objectives had been the French ATR-42 from SAFIRE, the German Falcon 20 from DLR, and the British Twin Otter from the British Antarctic Survey.

UCA (former UBP), SAFIRE (CNRS), UNIVMAN, UNIVLEEDS, and DLR all participated in measurements on the 3 aircraft, ensuring that instrumentation was calibrated and properly working.

The 3 aircraft performed in total 50 flight missions. Thereby, 23 flights were dedicated to aerosol-cloud interactions (thus dedicated to WP4), which corresponds to 70 h of data from all 3 aircraft. Out of these 70 flight hours, 32 h were conducted between Lomé and Savé, 10 h were spent in the region between Lomé and Kumasi, around 11 h of cloud sampling were carried out between Lomé and Abidjan, and remaining 17 h targeted broader regional objectives across the entire region sampled during DACCIWA flights.

After the end of the field project, the WP4 participants involved in the aircraft field project, focussed on the analysis and quality assurance of the data sets. The performed processing and quality assurance work involving UPMC, UCA (former UBP), UNIVMAN, SAFIRE (CNRS), and DLR is presented in this deliverable D4.3.

After a short introduction, this deliverable briefly presents aircraft core data (position, humidity, etc…) for all three aircraft. The subsequent main two sections then describe in sufficient detail the aerosol and cloud measurements, thereby presenting measurement instrumentation and derived aerosol and cloud parameters, data availability flight by flight, and finally the performed work to ensure high data quality.

2 Introduction

This deliverable details the quality controlled dataset for aerosol and cloud from the field campaign which took place between 25th June and 17th July. Three aircraft took part in the intensive campaign, all of which supported WP4 science, the ATR-42 of SAFIRE, France; the DLR Falcon; and the British Antarctic Survey Twin Otter. The delay of the intensive field phase by 12 months as a result of the 2015 Ebola outbreak in West Africa meant that the UK FAAM BAe-146, which was originally foreseen could not take part. This gap was resolved by commissioning the BAS Twin Otter aircraft to provide the 3rd aircraft platform. The Twin Otter is a smaller aircraft than the FAAM aircraft and its range and altitude are reduced. Its operating costs are cheaper than the BAe-146, but unlike the larger aircraft the Twin Otter was provided with very little science instrumentation fitted to it. UNIVMAN spent 5 months working with BAS to design, construct and test a new aerosol and cloud fit for WP4 in advance of the field experiment. This was successfully completed to ensure that all the key measurements for WP4 required were made on the Twin Otter. SAFIRE (CNRS) and DLR prepared the ATR-42 and Falcon aircraft and the instrumentation for the field intensive. UCA (former UBP) were also involved in preparing instrumentation for the ATR-42. UCA (former UBP) focussed on the final planning of the airborne campaign and the scientific operations in advance of the deployment.

During the intensive experiment UPMC, UCA (former UBP), UNIVMAN, UNIVLEEDS, KIT and DLR all participated in flight planning. UCA (former UBP), SAFIRE (CNRS), UNIVMAN, UNIVLEEDS, and DLR all took part in making measurements on the 3 aircraft, ensuring that instrumentation was calibrated and working and carried out aircraft scientific leadership during the missions. SAFIRE (CNRS/Météo France) coordinated the operational activities with the airport, local service providers, and aviation authorities in the different operating countries to allow access to the 3 aircraft.

The aircraft intensive experiment was very successful and has delivered considerable data for WP4. The 3 aircraft flew 50 missions in the period between 29th June 2016 and 16th July 2016. In total 23 flights were dedicated to aerosol-cloud interactions, amounting to 70 h of data from all 3 aircraft. Of these, 32 h were conducted on the sampling line between Lomé and Savé, 10 h were spent in the region between Lomé and Kumasi, around 11 h of cloud sampling was carried out between Lomé and Abidjan, and around 17 h of WP4 focussed activity took place more broadly across the region. In addition to these dedicated flights, a number of other flights contained sampling relevant to WP4 objectives. This is detailed in Deliverable D4.1 “The Summary Document for the Aerosol Cloud Campaign”. The document was prepared by UMPC and UNIVMAN and involved input from UPMC, UCA (former UBP), UNIVMAN, UPMC, SAFIRE (CNRS), and DLR.

Following the experiment, the WP4 team focussed on analysis and quality assurance of the data sets. This is currently ongoing and involves UPMC, UCA (former UBP), UNIVMAN, SAFIRE (CNRS), and DLR. To coordinate this activity and develop a strategy for combining the data and identify coordinating papers a meeting was held on 13th-14th October 2016 in Paris. UPMC, UCA (former UBP), UNIVMAN, SAFIRE (CNRS) and DLR took part in this meeting and also attended the annual Meeting in Leeds on 2nd-4th November 2016

3 Aircraft core data

3.1 ATR42

- Aircraft measurements were performed aboard the ATR-42, a French national research aircraft operated by SAFIRE (French aircraft service for environmental research). The ATR-42 basic instrumentation provides meteorological parameters including temperature, dew point temperature, pressure, turbulence, relative humidity, wind speed, direction, etc...

ATR-42 standard measurements			
Parameter	Instrument	Technique	Responsible institution
Wind direction & speed / TAS; position	AIRINS	INS + GPS: Inertial-GPS coupled navigation system.	SAFIRE
T	Rosemount	standard	SAFIRE
P static & dynamic	Rosemount 120 & 1221	standard	SAFIRE
Momentum & heat fluxes	5 port turbulence probe	standard	LA (UPS)
Humidity	GE hygrometer, KH20	Dew point mirror (GE), UV absorption (KH20)	LA (UPS) / SAFIRE
VIS radiances + fluxes up & down	Kipp & Zonen CMP22	standard	SAFIRE
IR radiances + fluxes up & down	Kipp & Zonen CGR4	standard	SAFIRE

Table 3-1 ATR-42 standard measurements

3.2 F20

- Meteorological measurements were performed aboard the DLR Falcon 20 by the meteorological data acquisition system (Malaun et al., 2015). Thereby the basic instrumentation includes data of the ambient temperature, dew point temperature, absolute water concentration, relative humidity, pressure, turbulence, wind speed, direction, bending angles. The meteorological data set of the Falcon is complete and has been submitted to the Server.

Date 2016 day/month	29/JUNE	30/JUNE	01/JULY	05/JULY	06/JULY	07/JULY	08/JULY	10/JULY	11/JULY	12/JULY	13/JULY	14/JULY
take off (hhmmss)	131134	112032	111328	112502	094416	110152	083429	110642	103004	083118	091822	085602
take off (hhmmss)	152034	145201	142907	145720	131237	133457	120922	143846	141423	121828	124307	123339
Flight #	Flight 8	Flight 9	Flight 10	Flight 13	Flight 14	Flight 15	Flight 16	Flight 17	Flight 18	Flight 19	Flight 20	Flight 21
CMET data	archived	archived	archived	archived	archived	archived	archived	archived	archived	archived	archived	archived
Routing	Lomé-Save-Lomé	Lomé-Accra-Takoradi-Kumasi-Lomé	Lomé-Accra-Kumasi Lomé	Lomé-Save Lomé	Lomé-Abidjan-Lomé	Lomé-Accra-Lomé	Lomé-Lomé	Lomé-Takoradi-Jubilee Lomé	Lomé-Abidjan-Espoir Lomé	Lomé-Lomé	Lomé-Lomé	Lomé-Accra-Jubilee Lomé

-

Table 3-2 Meteorological data status on board Falcon20 status according to flight mission

3.3 TO

- Total Temperature was measured by two Goodrich Rosemount Probes mounted on the nose. A non-de-iced model 102E4AL and a de-iced model 102AU1AG. These have compared well to other measurements on this and other aircraft.
- Static and dynamic pressure were measured using Honeywell precision altimeters in the aircraft static ports and heated Pitot tube on the co-pilot's side. It is recommended that the true air speed calculated using the BAT probe is normally used as it is thought to be more accurate.
- Several instruments were used to measure humidity. A Buck 1011C cooled mirror hygrometer was fitted on the aircraft nose on the co-pilot's side. This is not routinely calibrated but is compared with the on board Licor and during wing tip to wing tip with other research aircraft. A Licor LI 7000 CO2/H2O analyser was fitted primarily to measure fast humidity for calculating sensible heat fluxes. It can also be used as a backup for the other humidity instruments and is regularly compared to the Buck hygrometer. Relative humidity was measured by a Vaisala HMP110 humicap fitted to a Rosemount inlet. The pressure in the inlet was measured using a Vaisala PTB100B pressure sensor. This is used as a backup to Buck frost point hygrometer.
- Data were recorded from the aircraft's two Honeywell KRA 405B radar altimeters fitted in the tail section. Data are validated by comparison with a laser altimeter, though this was not fitted during DACCIWA but checked during the previous campaign. These have a range of around 1100m and a wider beam compared to a laser altimeter.
- Around 5m position accuracy was recorded from the JAVAD 4-antenna GPS attitude system. This system also records heading, pitch and roll at 20 Hz and velocities at 10 Hz. Aircraft attitudes and rate of change are recorded from the aircraft avionics Litef AHRS system. There is also an OXTS Inertial+ GPS linked INU available, which stores data internally.
- A NOAA/ARA Best Aircraft Turbulence (BAT) probe was fitted on a boom extending out from the roof of the aircraft on the co-pilot's side of the aircraft. This 9 hole probe recorded pressures and exposed thermocouple temperatures for measuring turbulence by eddy covariance in conjunction with attitude measurements. 3-axis accelerometer data were also recorded from the BAT Probe. This is a nine hole probe, one hole measuring static pressure, four measuring differential pressure and one static and this is used, along with an inertial navigation system to calculate the three wind components relative to the ground at 50Hz. This probe also measured fast temperature (at 50hz) using a fine wire thermocouple. The probe output was calibrated using aircraft manoeuvres during a flying campaign in December 2015.
- Two Sony DV-tape cameras were used. One downwards looking mounted in the camera hatch and one forward looking mounted in the cockpit.
- A pair of Eppley PIR and PSP sensors were fitted on the roof towards the rear of the aircraft, and a matching pair of Eppley PIR and PSP sensors were fitted to the camera hatch panel towards the rear of the aircraft facing downwards. Data are recorded at around 10 Hz. These instruments are used in work package 5 and are discussed in D5.2.

4 Aerosol properties

4.1 ATR42

4.1.1 Instrumentation product and data availability

The ATR-42 was particularly equipped to perform measurements of particles and gas phase species as well as cloud droplet size distribution. Aerosol particle species were sampled through a forward-facing inlet installed in place of a side window of the aircraft. This was an isokinetic and isoaxial inlet with a 50 % sampling efficiency for particles with a diameter of 4.5 µm. The inlet was composed of an outer sleeve for channelling air and a tube radius of curvature high enough to limit losses during transport of particles (Crumeyrolle et al., 2008).

4.1.1.1 GRIMM OPC 1.109 and 1.129

A GRIMM OPC (model sky-OPC 1.129) has been operated inside the cabin at a 1 s time resolution for measuring the optical size distributions between 0.25 and 2 µm on 16 size classes in nominal diameter. A second GRIMM OPC model 1.109) operated inside the cabin at a 6 s time resolution for measuring the optical size distributions between 0.3 and 32 µm on 32 size classes in nominal diameter. However, only data at nominal size below 12 µm were considered here due to the passing efficiency of the aerosols inlets connected to the GRIMM. Both instruments integrate light scattering between 30 and 150◦ at 655 nm. According to the calibration of the GRIMM OPC with size-standard particles, we assumed an uncertainty in diameter of 10 %.

4.1.1.2 CAPS, PSAP, and AURORA 3000

The particle extinction coefficient (σext) was measured with a cavity attenuated phase shift particle light extinction monitor (CAPS-PMex, Aerodyne Research) operated at the wavelength of 530 nm. The instrument relies on measuring the average time spent by the light within the sample cell that has an optical path length of 1–2 km. The sampling volumetric flow rate was 0.85 L min−1 and data were processed with a time resolution of 1 s. Uncertainty in σext measured with the CAPS is estimated to be 3 % (Massoli et al., 2010). The particle scattering coefficient (σscat) was measured at three wavelengths (450, 550 and 700 nm) with an integrating nephelometer (AURORA, model 3000), which integrates light scattered by particles at scattering angle between 9 and 170° relative to the incident and scattered radiation. The instrument also provide the particle back-scattering coefficient (σbackscat) measured at three wavelengths (450, 550 and 700 nm) for scattering angle between 90 and 170°. The instrument operated at a volumetric flow rate of 15 L min−1 and the data were acquired at 60 s time resolution. The instrument was calibrated with free-particle air and high-purity CO2 prior to and after the campaign. Uncertainty in σscat measured with the nephelometer is estimated to be 5 % (Muller et al., 2011a). For black carbon (BC) measurements, a particle soot absorption photometer (Radiance research® (PSAP) measured the particle absorption coefficient. The sampling flow rate of the PSAP was ~ 1.2 L min−1. Instrument time resolution of the PSAP was < 10 s. Light absorption coefficient was corrected according to the Bond et al. (1999) method. Filters were changed prior to each flight to ensure that transmission efficiency was greater than 80 %. Black carbon concentration were calculated using the light absorption coefficient at 650 nm and a mass specific absorption coefficient of QBC = 6.6 m2 g −1. This calculation was done in accordance with conclusions from a workshop (EUSAAR 2007) on the comparison of different measurements of absorption coefficient, and with the assumption that BC always interacts the same way with light whatever the BC particle's size. It has been illustrated in several studies that the majority of BC mass is measured in the submicron size mode (Sellegri et al., 2003).

4.1.1.3 SP2

The mass concentration of refractory black carbon particles (rBC) was measured using a single particle soot photometer (SP2, DMT). The SP2 uses a continuous intra-cavity Nd:YAG laser at the wavelength of 1064 nm to heat rBC containing particles to their vaporization point. Single particle rBC mass was derived from the peak intensity of the thermal radiation emitted by the incandescent rBC detected by the SP2. This method allows the quantification with 100 % efficiency of rBC mass in single particles with mass equivalent diameters between 80 and 500 nm (Moteki and Kondo, 2010). The total rBC mass loading was reported as the sum of all the detected single particle rBC masses. Prior to the measurement field campaign, the SP2 was calibrated using fullerene soot particles, which have been shown to give similar SP2 response as ambient rBC (Moteki and Kondo, 2010; Baumgardner et al., 2012; Laborde et al., 2012).

4.1.1.4 CPC MARIE and SMPS

The particle number size distribution was measured over the largest possible size spectrum by combining optical and electrical mobility techniques. The number size distribution in the submicron range was measured with an in-cabin scanning mobility particle sizer (SMPS). The SMPS consisted of a differential mobility analyser (DMA, Villani et al., 2007) interfaced to a condensation particle counter (CPC, TSI model 3010). A closed-loop recirculation was used for the sheath flow of the DMA. The SMPS system provided the number size distribution of the electrical mobility diameter from the 20–500 nm in 90 nominal size classes (i.e. size classes provided by the instrument not corrected for the dynamic shape factor) over time scans lasting 90 s (measurement) plus 30 s (down time). Data were processed by taking into account the particle electrical charging probabilities, the CPC counting efficiencies, the DMA transfer functions and the diffusion losses in the SMPS and CPC systems. The total number concentration of particles larger than 5 nm in diameter was measured using a butanol-based condensation nucleus counter (CPC, TSI model 3075) corrected for coincidences. The number concentrations derived from SMPS plus OPC are compared with total concentration from a Condensation Particle Counter (CPC 3010, TSI), which measured particles with diameter greater than 10 nm. In the overlap region, only SMPS measurements were considered. In general, the comparisons between OPC and SMPS concentrations in the overlap region reveals good agreement.

4.1.1.5 CCN counter

CCN measurements were made by using a mini-CCNC (Rober and Nenes, 2005). During the campaign it was operated in two modes: (i) at constant flow rates and temperature differences over the activation column, for measuring at a supersaturation of 0.15% or 0.25% and (ii) by continuously scanning the flow rate and temperature difference, for measuring in a range of supersaturations from 0.07 up to 0.53%.

4.1.1.6 Aerodyne AMS

Before aerosol particles were sampled by the compact time-of-flight aerosol mass spectrometer (C-ToF-AMS), they passed through a pressure controlled inlet (PCI). The PCI ensured a constant pressure at the inlet of the C-ToF-AMS (~ 400 hPa), avoiding pressure changes to the aerodynamic inlet of the C-ToF-AMS during airborne sampling (Bahreini et al., 2008). The aerodynamic lens of the C-ToF-AMS is reported to have a 100 % transmission efficiency between 80 nm and 500 nm when using a 100 µm orifice at 1016 mbar (Liu et al., 2007). Bahreini et al. (2008) illustrated when using a PCI between ~ 400 and 654 mbar (assuming that ambient pressure is greater than that of the PCI) with an orifice > 100 µm that the transmission efficiency of the lens is not changed. Bahreini et al. (2008) tried a number of different critical orifices ranging from 120 µm up to 180 µm; an orifice of 130 µm diameter was used in this study. Data acquired from the C-ToF-AMS as well as all other measurements aboard are corrected to temperature (~ 22 ◦C) and pressure (950 mbar) of the plane.

4.1.1.7 Airborne PCASP

A Passive Cavity Aerosol Spectrometer Probe (PCASP 100-X, Droplet Measurement Technology (DMT)), was operated outside the aircraft fuselage. The PCASP measures in the range 100 < Dp < 3000 nm over 30 channels. The PCASP is regularly calibrated at DMT with latex spheres (refractive index 1.59). PCASP measures dry aerosol particles sizes, since working with dry sheath air. In principle, because of the aerosol refractive index variability, PCASP data have to be corrected based on the Lorentz-Mie theory (Bohren and Huffman, 1983).

4.1.1.8 LIDAR

The mini backscattered lidar system ULICE operated in a nadir-viewing mode onboard the ATR 42. ULICE is a dual polarization, eye-safe lidar system operating at 355 nm with an output energy of 6mJ at 100 Hz (Shang and Chazette, 2014). It performed aerosols measurements over the Gulf of Guinea region. A variety of aerosol origins and properties were identified by using the coupling between the lidar cross-polarized channels and with in situ and other remote sensing data acquired on-board the ATR42.

4.1.2 DATA AVAILABILITY

Table 4-1 details aerosol instrumentation product and data availability for the ATR42 aircraft according to flight missions. The list includes aerosol concentration (CPC), size distribution (Grimm, SMPS, PCASP), chemical composition (AMS), cloud condensation nuclei (CCNC) and optical properties (CAPS, SP2, Aurora and PSAP).

Table 4-1 ATR-42 aerosol products and availability: Aerosol instrumentation onboard ATR42 status according to flight mission. Green color: archived, red color: no data, and yellow color: work is ongoing.

Date	29/Jun	30/Jun	01/Jul	02/Jul	02/Jul	03/Jul	05/Jul	06/Jul	06/Jul	07/Jul	08/Jul	08/Jul	10/Jul	11/Jul	11/Jul	12/Jul	13/Jul	14/Jul	15/Jul	16/Jul
TAKE-OFF TIME	135948	123641	102234	094049	144535	094224	080236	070838	124758	131650	054431	104000	101802	071011	133137	133830	122453	112923	092051	113424
LANDING TIME	164904	160901	134919	130423	180700	131318	105603	104931	150250	164940	091714	140417	135615	104758	162143	165845	155118	144554	124424	145340
Instrument / Property	Flight17	Flight18	Flight19	Flight20	Flight21	Flight22	Flight23	Flight24	Flight25	Flight26	Flight27	Flight28	Flight29	Flight30	Flight31	Flight32	Flight33	Flight34	Flight35	Flight36
Grimm109 (PSD 0.3-32 µm)	Archived	Archived	Archived	Archived	Archived	Archived	Archived	Archived	Archived	Archived	Archived	Archived	Archived	Archived	Archived	Archived	Archived	Archived	Archived	Archived
CAPS (Extinction)	Archived	Archived	Archived	Archived	Archived	Archived	Archived	Archived	Archived	Archived	Archived	Archived	Archived	Archived	Archived	Archived	Archived	Archived	Archived	Archived
SP2 (Black Carbon content)	Archived	Archived	Archived	Archived	Archived	Archived	Archived	Archived	Archived	Archived	Archived	Archived	Archived	Archived	Archived	Archived	Archived	Archived	Archived	Archived
SMPS (PSD 0.02-0.5 µm)	Achived	Achived	Achived	Achived	Achived	Achived	Achived	Achived	No data	Achived	Achived	Achived	Achived	Achived	No data	No data	No data	No data	No data	No data
Grimm129 (PSD 0.3-3 µm)	On going compar. with PCASP	On going compar. with PCASP	On going compar. with PCASP	On going compar. with PCASP	On going compar. with PCASP	On going compar. with PCASP	On going compar. with PCASP	On going compar. with PCASP	On going compar. with PCASP	On going compar. with PCASP	On going compar. with PCASP	On going compar. with PCASP	On going compar. with PCASP	On going compar. with PCASP	No data	No data	No data	No data	No data	No data
Aurora3000 (Diffusion @ 450, 525, 635 nm)	Achived	Achived	Achived	Achived	Achived	Achived	Achived	Achived	No data	Achived	Achived	Achived	Achived	Achived	No data	Achived	Achived	Achived	Achived	Achived
PSAP (Absorption @ 467, 530, 660nm)	Achived	Achived	Achived	Achived	Achived	Achived	Achived	Achived	No data	Achived	Achived	Achived	Achived	Achived	No data	Achived	Achived	Achived	Achived	Achived
Total Aerosol Particle Conc. (>10nm)	Achived	Achived	Achived	Achived	Achived	Achived	Achived	Achived	Achived	Achived	Achived	Achived	Achived	Achived	Achived	Achived	Achived	Achived	Achived	Achived
CCN concentration	See CNRM	See CNRM	See CNRM	See CNRM	See CNRM	See CNRM	See CNRM	See CNRM	See CNRM	See CNRM	See CNRM	See CNRM	See CNRM	See CNRM	See CNRM	See CNRM	See CNRM	See CNRM	See CNRM	See CNRM
Aerosol Chemical composition (AMS)	Achived	Achived	No data	No data	No data	Achived	Achived	Achived	Achived	Achived	Achived	Achived	Achived	Achived	Achived	Achived	Achived	Achived	Achived	Achived
PCASP (PSD 0.1-3 µm)	On going compar. with Grimm	On going compar. with Grimm	On going compar. with Grimm	On going compar. with Grimm	On going compar. with Grimm	On going compar. with Grimm	On going compar. with Grimm	On going compar. with Grimm	On going compar. with Grimm	On going compar. with Grimm	On going compar. with Grimm	On going compar. with Grimm	On going compar. with Grimm	On going compar. with Grimm	On going compar. with Grimm	On going compar. with Grimm	On going compar. with Grimm	On going compar. with Grimm	On going compar. with Grimm	On going compar. with Grimm
Cloud Presence (in, out, vicinity)	Achived	Achived	Achived	Achived	Achived	Achived	Achived	Achived	Achived	Achived	Achived	Achived	Achived	Achived	Achived	Achived	Achived	Achived	Achived	Achived

The ULICE lidar was operated during 7 flights, from 29 June to 3 July and from 14 to 15 July 2016. The lidar acquisition system crashed at the end of the flight on 5 July (data was lost) and was repaired on 13 July. The ULICE lidar raw data will be sent to the BAOBAB consolidated database before July 2017. More elaborate lidar data (extinction coefficient profiles, volume depolarization, etc.) are available upon request to Patrick Chazette (patrick.chazette@lsce.ipsl.fr).

4.1.3 Quality assurance and quality control

4.1.3.1 Aerosol number concentration (CPC)

The Condensation Particle Counter (CPC) provides aerosol concentration at 1Hz. The instrument has been calibrated in the laboratory prior campaign and its working parameters (e.g. condenser temperature) closely monitored. Aerosol concentration has been corrected applying an iterative coincidence algorithm.

4.1.3.2 Aerosol size distribution 20-500 nm (SMPS)

The Scanning Mobility Particle Sizer (SMPS) measures aerosol size distribution from 20 nm to 500nm every 120s. Quality assurance of this instrument focus on filtering out bad data (e.g. in cloud measurement where cloud droplets are spattered on the aerosol inlet and create artificial high concentration of particles) and comparison of integrated aerosol concentration with reference instrument, the CPC. Campaign-wide statistics for this instrument counted 1145 size distributions. From those measurements, quality control procedure largely relied on filtering out data considered bad or unreliable, according to the procedures described in Table 4.2 below:

Table 4-2 Quality assurance procedures applied to the 1145 measurement points gathered from the SMPS from the ATR42 aircraft during DACCIWA.

Filtering procedure	Remaining data points
1) On-flight zero checks or sampling clouds	876
2) Altitude change larger than 100m during scan	609
3) Inhomogeneous aerosol population (min CPC < 0.3* max CPC during scan) or large deviation (>100%) from CPC	531

Lastly, integrated aerosol concentration from the SMPS has been compared with an independent CPC. To avoid the impact of aerosols below 20nm, that would be measured by the CPC but not by the SMPS, only size distributions dominated by accumulation mode aerosols (70% of aerosol number between 100-500nm) were considered in the intercomparison. Through the comparison with the CPC, aerosol size distribution were multiplied by a scaling factor of 28%. Figure 4.1 depicts comparison of integrated aerosol concentration measured by the final SMPS data and the CPC, colored by geometric mean diameter.

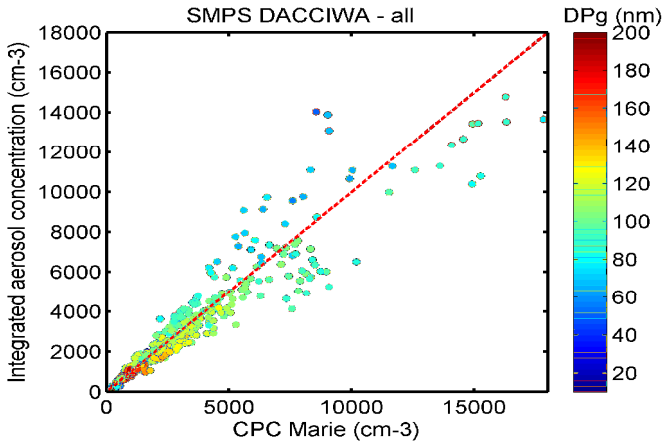

Figure 4-1 Scatterplot between integrated aerosol concentration from the SMPS and aerosol concentration from CPC coloured according the geometric mean diameter (Dpg)

4.1.3.3 Optical properties (Nephelometer, PSAP, CAPS)

The scattering results from nephelometer AURORA 3000 has been checked during the campaign using particle-free air and prior and after the campaign using a CO_2 standard. Corrections for truncation error were performed according to Müller et al., (2011b).

Aerosol absorption measured using the PSAP were carried out according to (Bond et al., 1999; Müller et al., 2011a), by applying a correction of air flow, the spot size, aerosol scattering (from the AURORA 3000) and removal of data where the transmission was above 1.05 or below 0.7. At last, data was smoothed using a Hanning function to reduce noise.

Prior to the campaign, the CAPS was evaluated against the combination of the nephelometer and the PSAP. The instrument intercomparison has been performed with purely scattering ammonium sulphate particles and with strongly absorbing black carbon particles. Both types of aerosols were generated by nebulizing a solution of the respective substances and size-selected using a DMA. For instrument intercomparison purposes, the extinction coefficient from the nephelometer + PSAP was adjusted to that for 530 nm by using the scattering and absorption Angtrom exponent. The instrument evaluation showed an excellent accuracy of the CAPS measurements by comparison to the nephelometer + PSAP combination. The level of uncertainty obtained for the test aerosol was beyond the upper limit of the CAPS uncertainty which was estimated to be +-3% according to Massoli et al. (2010).

4.1.3.4 Black carbon (SP2)

The SP2 was calibrated following the recommendations detailed in Laborde et al. (2012). The incandescence signal was calibrated (before, each week during and after the measurement campaign) using mobility size selected fullerene soot particles which is recommended for SP2 calibration as it gives similar SP2 responses as ambient rBC (Moteki and Kondo, 2010; Baumgardner et al., 2012;). The fullerene soot particles were selected by mobility diameter using a DMA and the corresponding particle masses were calculated using the effective density data provided in Gysel et al. (2011). The scattering signal was calibrated using monodispersed PSL spheres. The rBC mass in individual particles was determined from the peak intensity of the incandescence signal applying the fullerene soot calibration (Figure 4.2). The comparison of the calibration curves highlights a very good reproducibility of the rBC calibration during the campaign, reflecting a negligible drift in the SP2 mode aperture alignment.

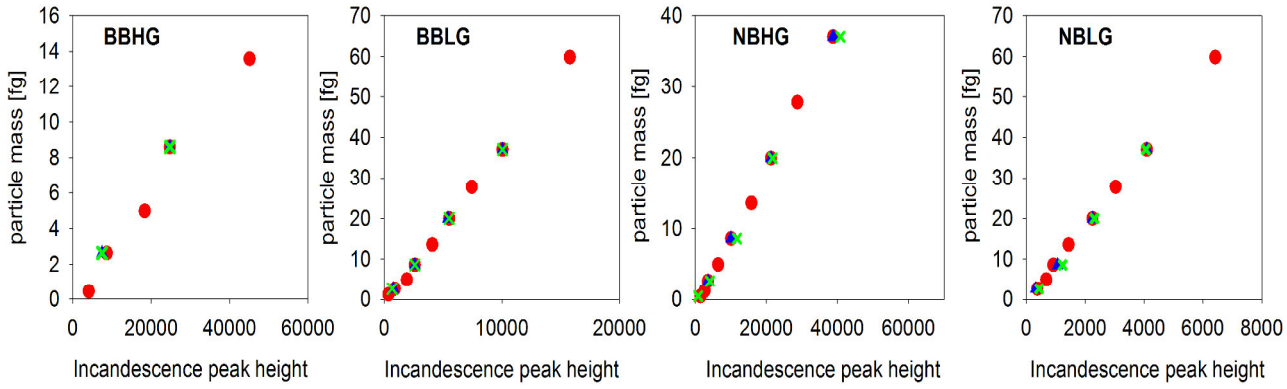

Figure 4-2 Comparison of fullerene soot calibrations of the broadband and narrowband incandescence detector for the low-gain and high-gain outputs obtained on 1 July (red), 8 July (green) and 15 July (blue).

4.1.3.5 Non-refractory submicrometric aerosol composition (AMS)

The AMS was calibrated four times during the field campaign by using size-selected (100, 200 and 300 nm) ammonium nitrate aerosols, and a time-dependent calibration factor was derived and applied to individual flights. Adjustments to the instrument fragmentation table were made based on particle-free measurements performed during each flight. The collection efficiency has been calculated according to Middlebrook et al., (2012), usually yielding 0.5. Data acquired from the AMS was corrected to temperature (~ 22◦C) and pressure (950 hPa) of the plane.

Aerosol loadings from the AMS estimates were compared against volume integration using the SMPS and Black Carbon from a SP2. The density used for each species was 1.78, 1.72, 1.72, 1.52, and 1.77 g cm^{-3} for sulphate, nitrate, ammonium, chloride, and BC, respectively (Holden and Lide, 1991; Park et al., 2004). The density of organics was estimated based on the oxygen-to-carbon (O : C) and hydrogen-to-carbon (H : C) ratios (Kuwata et al., 2012). Figure 4.3 depicts the comparison between the sum of the species measured by the AMS and integrated aerosol mass concentration from the SMPS minus BC using SP2 data.

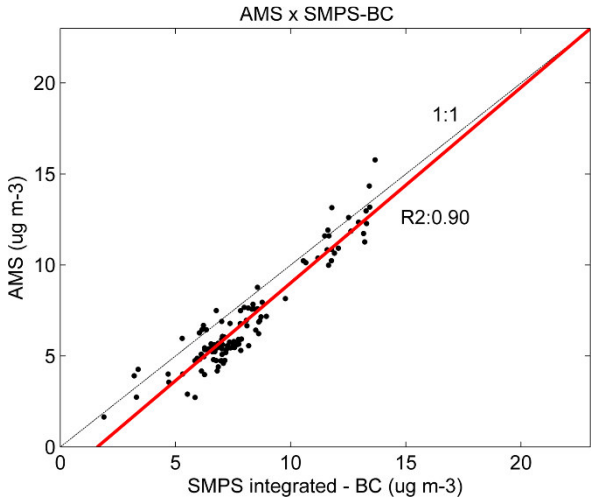

Figure 4-3 Scatterplot between the sum of the species measured by the AMS (organics, sulphate, nitrate, ammonium and chloride) and integrated aerosol mass concentration from the SMPS minus BC using SP2 data. Aerosol mass concentration from the SMPS has been calculated using an average aerosol density based on the fraction of the identified species, see text for details.

4.1.3.6 Cloud Condensation Nuclei activity

The supersaturation of the mini-CCNC was calibrated using size-selected ammonium sulfate particles prior and after the field measurement campaign. Experiments have been performed under a wide range of instrument operating conditions (5–8 K gradient temperature, 100–200 L min−1 flow rate). The CCN activation fraction (NCCN/NCN), was calculated from the concentrations of NCCN and NCN measured with a CPC and obtained from each particle diameters at constant temperature and flow rate. For each set of conditions, the effective water vapour supersaturation was determined from the measured CCN activation and Kohler model calculations.

Quality assurance of the mini-CCNC was performed by discarding data points where the total flow rate and the internal pressure deviate from the target values. In addition, NCCN values higher than the integrated aerosol concentration NCN were filtered out.

4.1.3.7 LIDAR

The quality of the lidar data acquired during DACCIWA was checked using parts of the ATR 42 flights made at higher altitude (> 5 km), i.e. above dust or biomass burning aerosol layers. Some pre-DACCIWA flights (e.g. during STRAP over the Mediterranean) were used as well. The quality assurance mainly consisted of verifying that when the aircraft was flying above aerosol layers, the lidar signal only consisted of molecular backscatter. This procedure also allowed setting up the calibration protocol for deriving the particle volume depolarization (based on cross-polarization measurements) and the geometrical factor (to correct extinction coefficient profiles). Comparison between lidar-derived and in situ-derived extinction profiles is ongoing.

4.2 F20

4.2.1 Instrumentation product and data availability

The DLR Falcon 20 was equipped with an extensive payload to measure trace gases, aerosols and cloud hydrometeors. Instruments were located in the cabin behind suitable inlet systems and, for larger particles, mounted outside in under-wing carriers. The gas-phase instrumentation will be discussed elsewhere. The aerosol instruments inside the fuselage all draw their sample air from the Falcon aerosol inlet on a zenith aperture plate toward the rear of the aircraft. All samples were drawn through the forward-facing inlet sample line which provides iso-axial and near-isokinetic sampling for normal flight conditions. The cut-off size for large particles for this inlet is between 1.5 and 3µm depending on flight altitude.

Table 4-3 Overview on data availability for aerosol instrumentation and products

Date	29 JUNE	30 JUNE	01 JULY	05 JULY	06 JULY	07/JULY	08 JULY	10 JULY	11 JULY	12 JULY	13 JULY	14 JULY
take off (hhmmss)	131134	112032	111328	112502	094416	110152	083429	110642	103004	083118	091822	085602
take off (hhmmss)	152034	145201	142907	145720	131237	133457	120922	143846	141423	121828	124307	123339
Flight #	Flight 8	Flight 9	Flight 10	Flight 13	Flight 14	Flight 15	Flight 16	Flight 17	Flight 18	Flight 19	Flight 20	Flight 21
Flight ID	F20_160629a	F20_160630a	F20_160701a	F20_160705a	F20_160706a	F20_160707a	F20_160708a	F20_160710a	F20_160711a	F20_160712a	F20_160713a	F20_160714a
TSI3010	Archived	Archived	Archived	Archived	Archived	Archived	Archived	Archived	Archived	Archived	Archived	Archived
SkyOPC 0.25-2µm	Archived	Archived	Archived	Archived	Archived	Archived	Archived	Archived	Archived	Archived	Archived	Archived
SkyOPC 0.25-30µm	Expected by mid-June 2017	Expected by mid-June 2017	Expected by mid-June 2017	Expected by mid-June 2017	Expected by mid-June 2017	Expected by mid-June 2017	Expected by mid-June 2017	Expected by mid-June 2017	Expected by mid-June 2017	Expected by mid-June 2017	Expected by mid-June 2017	Expected by mid-June 2017
UHSAS-A	Data analysis ongoing	Data analysis ongoing	Data analysis ongoing	Data analysis ongoing	Data analysis ongoing	Data analysis ongoing	Data analysis ongoing	Data analysis ongoing	Data analysis ongoing	Data analysis ongoing	Data analysis ongoing	Data analysis ongoing
PCASP	Data analysis ongoing	Data analysis ongoing	Data analysis ongoing	Data analysis ongoing	Data analysis ongoing	No data	No data	No data	No data	No data	No data	No data
AMS	Data analysis ongoing	Data analysis ongoing	Data analysis ongoing	Data analysis ongoing	Data analysis ongoing	Data analysis ongoing	Data analysis ongoing	Data analysis ongoing	Data analysis ongoing	Data analysis ongoing	Data analysis ongoing	Data analysis ongoing
F20 Met data	Archived	Archived	Archived	Archived	Archived	Archived	Archived	Archived	Archived	Archived	Archived	Archived

4.2.1.1 Condensation particle counter TSI 3010

To measure total aerosol particle number concentration a butanol-based, heavily modified condensation particle counter (TSI Inc, model 3010) was used. In addition to the standard setup of the counter a switch has been integrated to control the saturator temperature to shift the lower cut-off diameter towards smaller sizes. The cut-off of this counter has been determined in lab measurements to be around 14nm. The CPC was connected to a 4.66m long stainless steel sample line inside the cabin. To minimize particle losses in the sample line a bypass was used to accelerate the airflow through the tubing. The particle transmission efficiency is estimated to be above 90% for particle diameters between 10nm and 1.5µm. The particle counter performed well during all flights. Concentration data in (ambient and STP corrected) in 1Hz time resolution merged with aircraft basic position and meteorological data are available for all flights in final form.

4.2.1.2 Grimm SkyOPC

The Falcon20 had two optical particle counters SkyOPC (Model 1.129) by Grimm Aerosol Technik, Ainring, Germany integrated inside the cabin behind the Falcon isokinetic inlet system. One of the OPC operated in multiplex mode, i.e. sampling the size range from 250nm to 30µm every 6s, the other one was operated at 1Hz time resolution with a size range of 250nm to ~2.5µm. The sample air was drawn though a 2.1m and 2.6m long stainless steel tubing, respectively. The transmission efficiency for the inlet and tubing is expected to be above 95% up to ~1.5µm depending on flight altitude. For larger particles the transmission efficiency is expected to drop substantially. Time series of channel concentrations together with bin appropriate threshold diameters (PSL equivalent) are reported for the SkyOPC. All data are corrected for stp conditions.

4.2.1.3 UHSAS-A

The Ultra-high Sensitivity Aerosol Spectrometer, Airborne (Manufacturer: Droplet measurement technologies, Boulder, CO, USA) is a wing-mounted optical particle spectrometer with an intra-cavity measurement at a wavelength of 1.054µm. The nominal diameter range reaches from 60nm to 1µm detected in up to 99 adjustable size bins. During DACCIWA the instrument did not perform ideally such that reliable size measurements are only possible between ~100nm and ~500nm. The spectrometer is also fairly sensitive to overheating which affects the quality of the laser beam in the measurement cavity. The instrument measured during all flights but due to the high temperatures encountered during the DACCIWA measurement flights only part of the data will be useable. On 3 July 2016 the laser was found to be in an unstable mode probably due to accumulation of dirt in the optics. Therefore the laser parameters had to be readjusted requiring a complete recalibration of the gain stage overlaps. Data analysis and quality assurance for the UHSAS-A is still ongoing. Final, quality-controlled time series data is expected by the 3rd quarter of 2017.

4.2.1.4 PCASP

The Passive Cavity Aerosol Spectrometer Probe 100X-SPP (Manufacturer: Droplet Measurement Technologies, Boulder, CO, USA) is also a wing-mounted aerosol spectrometer with inlet system measuring dry aerosol between 100nm and 3µm. Due to electronic problems with a logic board the instrument showed occasional connection failures leading to data gaps in the first part of the campaign. After the flight on 5 July no further data could be acquired. Data analysis for the PCASP is also still ongoing. Final data as far as it is available is expected in the 3rd quarter of 2017.

4.2.1.5 Aerosol mass spectrometer (C-ToF-AMS)

The chemical composition of the non-refractory fraction of the submicron aerosol particles was measured with a compact time-of-flight aerosol mass spectrometer (C-ToF-AMS). Aerosol particles entered the AMS after passing through a pressure controlled inlet (PCI). Unlike the AMS-PCI on the ATR42, the AMS-PCI on the Falcon keeps the pressure before the AMS inlet constant by

dynamically adjusting the inlet orifice cross section (Molleker et al., in preparation). The different designs of these PCIs may be at the root of the discrepancies in the aerosol masses that were observed by the different AMSs. After the appropriate calibrations and corrections are made, the resulting time series of particulate nitrate, ammonium, sulphate and organic matter mass concentrations will be made available on the database by the end of August 2017. Data acquired from the Falcon C-ToF-AMS are corrected to STP.

4.2.2 Quality assurance and quality control

Aerosol data drawn from the forward inlet are known to be affected by artefacts during measurements sequences inside clouds. This is particularly true for denser liquid-water and mixed-phase clouds. Therefore a cloud mask was derived based on measurements of condensed water content (Ch. Voigt, S. Kaufmann) and the cumulative concentration of particles detected in the CAS-DPOL instrument in bins 10 to 30 (corresponding to diameters of ~5 to 50µm). Data points inside clouds have been removed from the data set. Another potential cause of artefacts and unreliable data are flight situations where the air flow is not isoaxial to the inlet or fast changes in pressure occur. Specifically this applies to sequences where the aircraft makes tight turns or fast changes of altitude. Unisoaxial sampling leads to a distortion of the particle size distribution seen by the optical particle counters, fast ascents or descents in addition lead to temporarily unstable pressure and flow situations inside the measurements chambers such that the concentrations might not reflect the true ambient conditions until an equilibrium pressure in the system has been re-established. Therefore, all data have been screened and flagged for situations where the roll angle of the plane exceeds 7° and the climb or decent rate is larger than 200ft/min. The data inside those limits are marked as “on level” meaning that the data is expected to be reliable. Data points taken outside those boundary conditions have not been removed and might still be usable, however have to be treated with care depending on the application.

4.2.2.1 Integral particle number concentration (Condensation particle counter TSI 3010)

The particle concentrations have been derived based on the sample flow through the instrument measured before the start of the campaign and are corrected to both ambient and stp conditions using temperature and pressure measured in the sample line close to the instrument. The resulting raw counts are corrected for coincidence effects following the procedure suggested in the manufacturer’s manual. For particle concentrations above ~20000 cm^{-3} the coincidence correction becomes unreliable. Concentrations larger than this value have therefore been flagged and removed from the data set. The counting efficiency of the TSI3010 has been tested against a Faraday cup electrometer in the lab using NaCl aerosol generated in a furnace. At low ambient pressure the counting efficiency of drops by 5-15%. The overall measurement uncertainty for the TSI3010 is therefore expected to be within 15%.

4.2.2.2 Aerosol particle size distributions (Grimm SkyOPC, UHSAS-A, PCASP)

All OPC have been calibrated using Polystyrene Latex spheres (PSL) before the campaign and in between flight missions as far as time permitted to be able to account for shifts in the calibration caused e.g., by degrading laser power of accumulation of dirt and dust in the optics. Using the same cloud mask as for the CPC cloud sequences have been removed from the data set to avoid effects from cloud particle shattering in the inlet system. For the PCASP and UHSAS the time series have to be screened for artefacts caused by unstable laser conditions and detector noise due to temperature problems. The SkyOPC performed well even in a comparably high-temperature environment.

4.2.2.3 Non-refractory submicron aerosol composition (C-ToF-AMS)

The nitrate ionization efficiency (IE) of the C-ToF-AMS was determined with size-selected ammonium nitrate particles (200-350 nm) once before, once during, and several times after the campaign. Additionally, the sulphate relative ionization efficiency (RIE) was determined with ammonium sulphate particles during the field campaign. In-flight filter measurements were used to make adjustments to the instrument fragmentation table.

A comparison of the preliminary AMS data from the different aircraft showed that the Falcon AMS measured up to five times lower aerosol mass loadings than the other two AMSs, which may be due to the different PCI designs. A preliminary, altitude-dependent correction function has been derived; co-located aerosol measurements during the campaign and laboratory tests will be used to refine this correction.

4.3 TO

4.3.1 Instrumentation product and data availability

Aerosol was sampled on the Twin Otter by a suite of inboard instrumentation listed in Table 4-4. The PCASP was wing-mounted and was not fitted for all flights, as limited space on the pylon meant it had to be swapped out for the 2DS. The inboard aerosol probes sampled from a Brechtel model 1200 isokinetic inlet, with a dried sample flow. The inlet RH was measured between 20-40% in-flight. Data marked as archived in Table 4-4 have been uploaded to the DACCIWA SEDOO database. We recommend aerosol data are screened for clouds using the CDP data when analysed. The archived data for the inboard instruments are corrected to standard temperature (273.15 K) and pressure (1013.25 hPa). The outboard instruments are reported at ambient temperature and pressure.

Table 4-4 List of aerosol instrumentation mounted on the BAS Twin Otter aircraft

Date	01-Jul	03-Jul	04-Jul	05-Jul	05-Jul	06-Jul	06-Jul	07-Jul	08-Jul	08-Jul	10-Jul	10-Jul	11-Jul	11-Jul	13-Jul	14-Jul	15-Jul	15-Jul
Takeoff time (UTC)	1410	1101	1155	1124	1600	0942	1355	0946	0836	1330	0854	1418	0817	1215	0859	0655	0930	1340
Landing time (UTC)	1725	1400	1515	1245	1750	1140	1637	1241	1127	1635	1133	1615	1024	1445	1205	0925	1205	1645
Instrument / Property	TO01	TO02	TO03	TO04	TO05	TO06	TO07	TO08	TO09	TO10	TO11	TO12	TO13	TO14	TO15	TO16	TO17	TO18
AMS	Not archived	Not archived	Not archived	No data	Not archived	No data	Archived	Archived	No data	Archived	Archived	Archived	Archived	Archived	Archived	Archived	Archived	Archived
SP2	No data	Archived	No data	No data	No data	Archived	No data	No data	Archived	No data	Archived	Archived	Archived	No data	Archived	Archived	Archived	Archived
PCASP	No data	No data	No data	No data	Archived	No data	Archived	Archived	Archived	Archived	Archived	Archived	Archived	Archived	Archived	Archived	Archived	Archived
SMPS	Comparison ongoing	Comparison ongoing	Comparison ongoing	Comparison ongoing	Comparison ongoing	Comparison ongoing	Comparison ongoing	Comparison ongoing	Comparison ongoing	Comparison ongoing	Comparison ongoing	Comparison ongoing	Comparison ongoing	Comparison ongoing	Comparison ongoing	Comparison ongoing	Comparison ongoing	Comparison ongoing
UHSAS	Comparison ongoing	Comparison ongoing	Comparison ongoing	Comparison ongoing	Comparison ongoing	Comparison ongoing	Comparison ongoing	Comparison ongoing	Comparison ongoing	Comparison ongoing	Comparison ongoing	Comparison ongoing	Comparison ongoing	Comparison ongoing	Comparison ongoing	Comparison ongoing	Comparison ongoing	Comparison ongoing
GRIMM	Comparison ongoing	Comparison ongoing	Comparison ongoing	Comparison ongoing	Comparison ongoing	Comparison ongoing	Comparison ongoing	Comparison ongoing	Comparison ongoing	Comparison ongoing	Comparison ongoing	Comparison ongoing	Comparison ongoing	Comparison ongoing	Comparison ongoing	Comparison ongoing	Comparison ongoing	Comparison ongoing
CAPS PMssa	No data	Comparison ongoing	Comparison ongoing	Comparison ongoing	Comparison ongoing	Comparison ongoing	Comparison ongoing	Comparison ongoing	Comparison ongoing	Comparison ongoing	Comparison ongoing	Comparison ongoing	Comparison ongoing	Comparison ongoing	Comparison ongoing	Comparison ongoing	Comparison ongoing	Comparison ongoing
CPC	No data	Archived	No data	No data	No data	No data	Archived	Archived	No data	Archived	No data	No data	No data	Archived	No data	Archived	Archived	Archived
CCNC	No data	No data	No data	No data	No data	No data	No data	No data	No data	No data	No data	No data	No data	No data	No data	No data	No data	No data
TAP	Not archived	No data	No data	No data	No data	No data	No data	No data	No data	No data	No data	No data	No data	No data	No data	No data	No data	No data

4.3.1.1 SP2

The mass concentration of refractory black carbon particles (rBC) was measured using a Single Particle Soot Photometer (SP2, DMT), as for the other aircraft. This instrument is the same as is described in section 4.1.1. The total rBC mass loading was reported as the sum of all detected single particle rBC masses. Due to overheating inside the instrument, particularly during the afternoons, the SP2 was unable to gather data for several flights. We report the rBC mass concentration in the archived data, and users should contact the PI for higher level data products.

4.3.1.2 Aerodyne AMS

The Aerosol Mass Spectrometer (AMS) on board the Twin Otter aircraft was set up in a similar way to that on board the ATR, discussed in section 4.1.1. The incoming aerosol beam was collected from a Rosemount inlet on the aircraft. The instrument was calibrated before and after each flight using ammonium nitrate particles of known diameters, in order to convert measured signals into mass concentrations. The method used is outlined by Drewnick et al. (2007). Due to the long pre-flight pump down period required for the AMS to reach optimal performance (> 4 hrs.), it was not possible for the instrument to be running on all flights. For the first few flights (TO-01 – TO-05), the pinhole in the inlet of the AMS was partially blocked, so data from these flights is not representative and will therefore not be uploaded. The multichannel plate (MCP) in the AMS detection region was replaced after flight TO-10, so calibrations after this flight are likely to differ slightly from those before. Different calibrations were applied to ensure that the data is comparable.

4.3.1.3 GRIMM

A GRIMM model 1.109 was operated inside the Twin Otter cabin. This is the same instrument as described in Section 4.1.1. The instrument ran well throughout the campaign and no problems have yet been found with the data, though the comparison of sizing instruments is still ongoing.

4.3.1.4 UHSAS

The UHSAS-A is an optical spectrometer that measures the aerosol size distribution on a time resolution of 1 s. The distribution of scattered light is converted to optical-equivalent diameter using a Mie scattering table. The instrument ran on every flight, though it had a problem on some flights where the sample time was not measured correctly. This issue was corrected for after the campaign by comparing the measured concentrations to the other aerosol probes.

4.3.1.5 Airborne PCASP

A Passive Cavity Aerosol Spectrometer Probe (PCASP 100-X, with SPP200 electronics, Droplet Measurement Technology (DMT)), was operated in one underwing canister. The PCASP measures in the range 100 < Dp < 3000 nm over 30 channels. The PCASP is regularly calibrated at DMT with latex spheres (refractive index 1.59). PCASP measures approximately dry aerosol particles sizes, since samples are mostly dried by ram heating and by being enclosed in dry sheath air. In principle, because of the aerosol refractive index variability, PCASP data have to be corrected based on the Lorentz-Mie theory. The PCASP was calibrated once during the campaign on 15th July 2016 using PSL microspheres and the methods from Rosenberg et al (2012). The instrument uses three gain stages of different gains to measure over three different size ranges to make up its full range. Insufficient PSL microspheres were available to calibrate the first gain stage, which measures the smallest particles (channels 1-6). This method allows the user to correct the calibration for the effects of sample refractive index. Contact Phil Rosenberg or Jonny Taylor for details and software.

4.3.1.6 CAS

The CAS measures medium to large aerosol and cloud droplets in the size range 0.5-50 μm. It is part of the CAPS probe and was mounted in an underwing canister. Its open path sample area surrounded by a guide tube means particles are measured close to ambient condition.

4.3.1.7 CPC

A Brechtel model 1720 mixing condensation particle counter (mCPC) was used to count total aerosol concentration with a 1 s time resolution. The instrument ran on all flights but the data collected was of variable quality. The operators struggled were unable to determine how full the instrument's butanol reservoir was, and the auto-filling procedure often didn't work. Consequently, on some flights the butanol level was low enough that the instrument ran out partway through the flight, and on others the butanol level was so low that the instrument measured no particles for the whole flights. This issue was diagnosed by comparing the CPC concentration to the integrated concentration measured by the SMPS. A constant non-zero CPC/SMPS ratio meant the CPC counted efficiently for the whole flight (TO02, TO07, TO08, TO10, TO14, TO16, TO17, TO18); a decreasing ratio meant the CPC was running out of butanol; a near-zero ratio meant the CPC had run out of butanol.

4.3.1.8 SMPS

A custom-built SMPS was run by combining a TSI 3081 DMA with a TSI 3772 CPC, with an inlet flow rate of 1 L min^{-1}. The sheath flow was recirculated and controlled by an Alicat flow meter at 5 L min^{-1}. A filtered dilution flow of 0.5 L min^{-1} was introduced into the CPC's sample flow after the DMA to maintain a 10:1 sheath/sample ratio through the DMA, and this has been accounted for in the analysed data. The instrument ran size scans from 20 – 350 nm every 60s in 26 size bins. Occasionally, an error in the logging software caused a reduction in the number of size bins, but did not affect the size range. The bin diameter as well as the dN/dlogDp for each bin are provided as a function of time. The SMPS ran every flight but the data analysis is still ongoing, as is discussed further in the next section.

4.3.1.9 CCNC

A CCN counter the same as the one described in Section 4.1.1 was mounted on the Twin Otter for TO03-TO05, but no ambient data were measured and it was removed from the aircraft for maintenance. The instrument suffered from overheating and an electrical issue, and these were not resolved during the campaign despite determined efforts by the operators.

4.3.1.10 TAP

A Brechtel tricolour absorption photometer (TAP), similar to the PSAP described in section 4.1.1, was installed on the Twin Otter. Pre-flight procedures included changing the filter and preconditioning the new filter, but the preconditioning step failed on all but flight TO01. As the SP2 and PM_{SSA} were not functioning on this flight, we have thus far been unable to QA the data and it is therefore not of a sufficient quality to archive at the present time. We recommend anyone interested in the data contact the PI.

4.3.1.11 CAPS PMex

This instrument is the same as that described in section 4.1.1. The instrument and its setup are described by Massoli et al. (2009). During the earlier part of some flights, the instrument was sometimes unable to find a reliable baseline from which to calculate extinction and scattering values. As a result, the data collected from around the first half hour of some flights is unusable. A correction is currently being developed to account for the limited detection angles of the scattering detector. The data will be archived once this correction has taken place.

4.3.1.12 Filter samples

A total of 28 filter samples were taken over 9 flights, as well as 2 blanks, for analysis with an environmental scanning electron microscope with field-emission gun (ESEM-FEG) in partnership with an energy-dispersive X-ray spectroscopy (EDS) system. The flow rate through the filters was fixed at 30 L min^{-1} through a critical orifice. The start and end times of the samples are listed in Table 4.5. Analysis of the samples is currently ongoing.

Table 4-5 List of sampling times for the Twin Otter filter samples.

Flight	Date	Start time 1	End time 1	Start time 2	End time 2	Start time 3	End time 3	Start time 4	End time 4
TO-01	01/07/16	150735	152024	153800	154750	154956	155946	162902	163504
TO-02	03/07/16	111151	112114	120139	121013	123923	124807	135428	Ground ~1400
TO-03	04/07/16	125332	130748	131219	132445	133015	134618	134747	140352
TO-07	06/07/16	145727	150453	?	152452	152638	153341	153650	155435
TO-10	08/07/16	141226	142214	145130	150112	N/A	N/A	N/A	N/A
TO-11	10/07/16	91847	93115	100718	102047	Blank	Blank	Blank	Blank
TO-13	11/07/16	95355	101655	N/A	N/A	N/A	N/A	N/A	N/A
TO-14	11/07/16	N/A	N/A	130845	131958	132443	133533	133759	134914
TO-15	13/07/16	093300	095130	095300	101215	101340	105120	105555	111111

4.3.2 Quality assurance and quality control

4.3.2.1 AMS

The quality assurance for the AMS followed the steps recommended in the online Field Analysis Guide (http://cires1.colorado.edu/jimenez-group/wiki/index.php/Field_Data_Analysis_Guide). There were some small differences in the adjustments made to the fragmentation table for the two different MCPs used. Data before flight TO-06 was rejected due to the blocked pinhole. Sulphate and ammonium calibrations were used to adjust the sulphate and ammonium relative ionisation efficiency (RIE) to 1.4319 and 3.831 respectively.

4.3.2.2 SP2

The SP2 instrument's incandescence measurements were calibrated to black carbon mass using Aquadag (Aqueous Deflocculated Acheson Graphite) and following the approach of Laborde et al. (2012), with a correction factor of 0.75 applied. The instrument alignment was checked and scattering measurements were calibrated to particle size using monodisperse polystyrene latex (PSL) spheres. These calibrations were carried out at the start of the measurement campaign.

4.3.2.3 UHSAS, SMPS, PCASP and GRIMM

A comparison of the Twin Otter sizing probes is still ongoing. Here we describe QA carried out on the various sizing probes, and present a comparison of the derived distributions. The UHSAS sizing was checked at the start of the campaign using several sizes PSLs. These showed that the sizing was accurate within around 10%. The detection efficiency of the UHSAS is known to drop off at sizes below around 150 nm, though the exact cut-off point for 100% detection efficiency is unknown. The PCASP data were corrected for airspeed and the size bins were calculated as described in the previous section.

4.3.2.4 SMPS

SMPS data were filtered for periods where the instrument flows either changed during a scan or were not within 1% of their set points. An investigation comparing the SMPS integrated total concentration to the CPC concentrations showed that the SMPS appeared to be overcounting by a factor of ~3 on many flights. Tests using lognormal fits to the SMPS distribution showed the contribution of particles outside this size range was at most of the order of a few percent. The cause of this factor is currently unknown, though it is consistent during each flight. Figure 4.4 shows how these comparisons changed throughout the campaign. On some flights, the laser drive current on the SMPS CPC was also insufficiently low, which caused a drop in the SMPS counting efficiency. Figure 4.5 shows a comparison of all the different sizing probes. It is clear that normalising the SMPS to the CPC gives better agreement with the other probes. This comparison is still ongoing, but we anticipate that we will release normalised SMPS data in the near future.

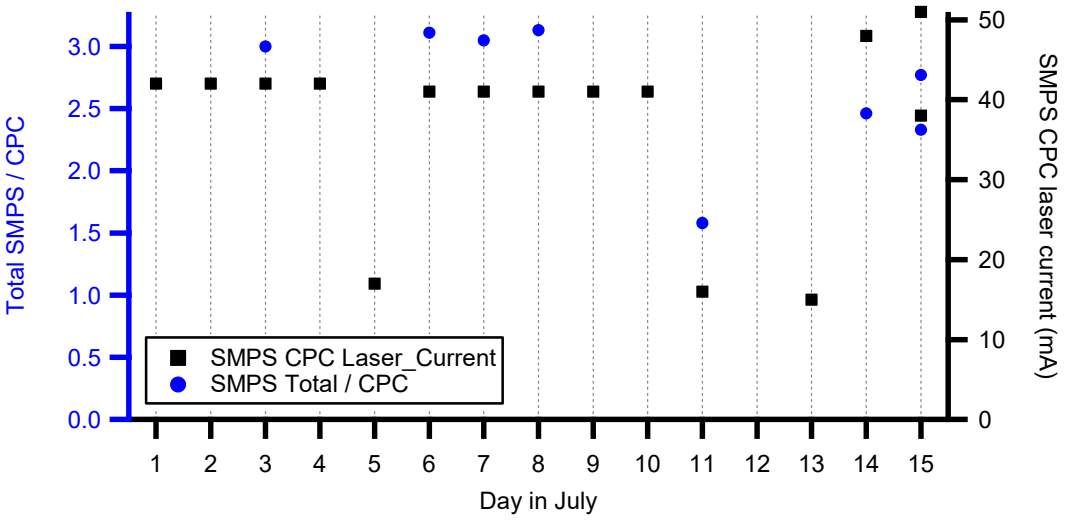

Figure 4-4 Time series of comparisons between the integrated total concentration measured by the SMPS to that measured by the CPC. Also plotted are the measured laser current from the SMPS CPC.

Comparing the other sizing instruments in Figure 4.5, some other differences are apparent. The UHSAS undercounts compared to the SMPS even when normalised. This is especially the case at smaller sizes, as is expected by the UHSAS's decreasing detection efficiency. The gain stage boundaries are also visible in the UHSAS size spectrum, such as the trough in concentration at 250 nm. As the PCASP was mounted outside the aircraft, the sample flow does not benefit from the drying in the inlet line as it enters the cabin, and the sizing is therefore somewhere between the wet and dry diameters. This may be the cause of some of the disagreement between the PCASP and the corrected SMPS and GRIMM. At the larger sizes, the shapes of the distributions from the GRIMM, UHSAS and PCSAP are similar until around 2 μm where the PCASP sees a coarse aerosol mode that is not apparent in the GRIMM. This may be due to a lower inlet efficiency

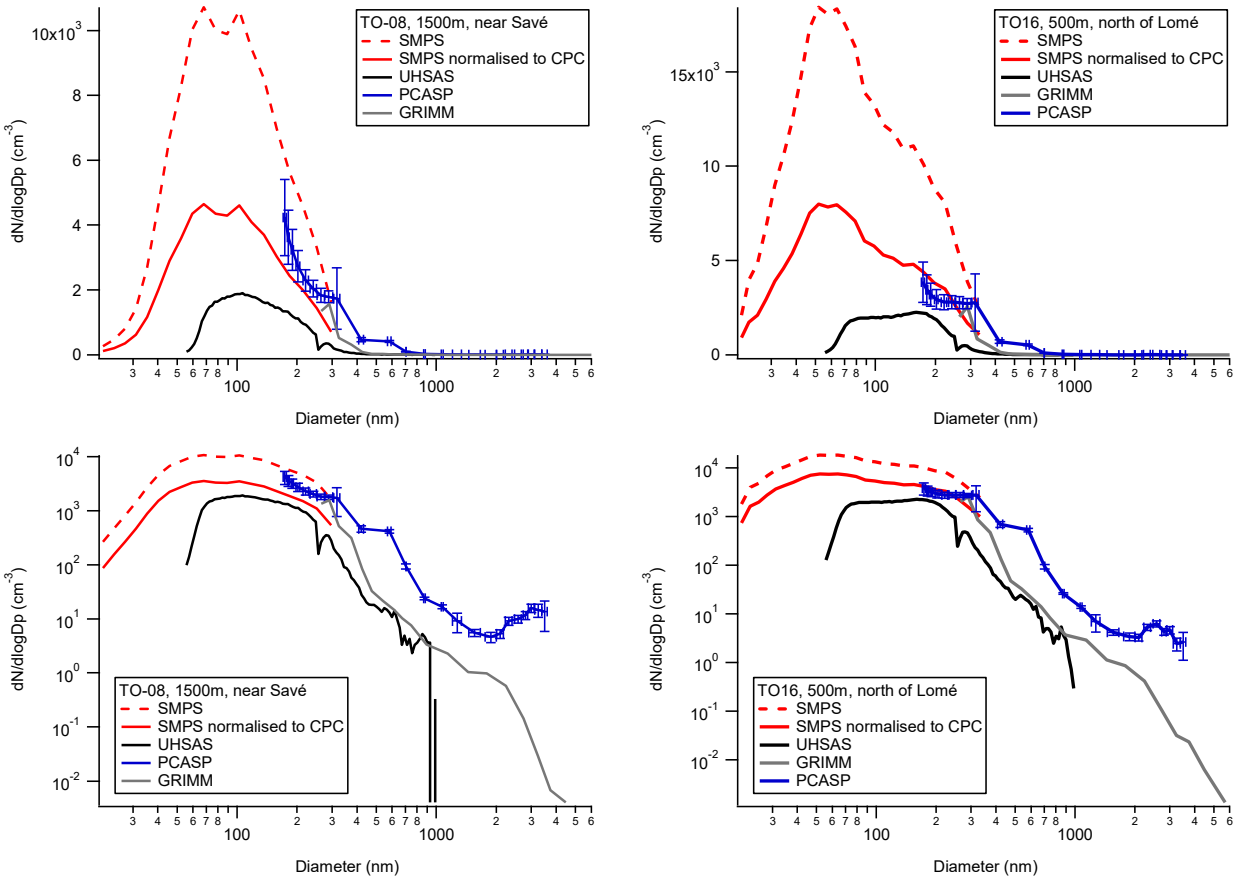

Figure 4-5 Comparison of different sizing probes from the BAS Twin Otter. The upper and lower panels show the same data, but with linear and logarithmic y-axes respectively.

5 Cloud properties

5.1 ATR42

5.1.1 Instrumentation product and data availability

The in situ microphysics package included a cloud droplet probe (CDP-2; DMT; Baumgardner et al. 2011), a FCDP (SPECinc,) and a 2D-stereo (2D-S; SPECinc ; Lawson et al. 2006). The CDP-2 (30 size bins) and FCDP (20 size bins) sampled the smallest cloud particle sizes from nominally 2 to 50 µm. The 2D-S was used to image and size from 10 to 1280 mm at 10-mm resolution. Thanks to image reconstruction, the 2D-S provides size information of particles larger than the nominal maximum particle size, up to 2560µm.

Table 5-1 Cloud instrumentation on board ATR42: status according to flight mission.

Date	29/Jun	30/Jun	01/Jul	02/Jul	02/Jul	03/Jul	05/Jul	06/Jul	06/Jul	07/Jul	08/Jul	08/Jul	10/Jul	11/Jul	11/Jul	12/Jul	13/Jul	14/Jul	15/Jul	16/Jul
TAKE-OFF TIME	135948	123641	102234	094049	144535	094224	080236	070838	124758	131650	054431	104000	101802	071011	133137	133830	122453	112923	092051	113424
LANDING TIME	164904	160901	134919	130423	180700	131318	105603	104931	150250	164940	091714	140417	135615	104758	162143	165845	155118	144554	124424	145340
Instrument / Property	Flight17	Flight18	Flight19	Flight20	Flight21	Flight22	Flight23	Flight24	Flight25	Flight26	Flight27	Flight28	Flight29	Flight30	Flight31	Flight32	Flight33	Flight34	Flight35	Flight36
2DS (PSD 30-2560 µm)	Archived	Archived	Archived	Archived	Archived	Archived	Archived	Archived	Archived	Archived	Archived	No Data	Archived	Archived	Archived	Archived	Archived	Archived	Archived	Archived
CDP/FCDP (PSD 2-50 µm)	Archived	Archived	Archived	Archived	Archived	Archived	No Data	No Data	No Data	No Data	Archived	Archived	Archived	Archived	Archived	Archived	Archived	Archived	Archived	Archived
FCDP (PSD 2-50 µm)	Not Archived	Not Archived	Not Archived	Not Archived	Not Archived	Not Archived	Archived	Archived	Archived	Archived	Not Archived	Not Archived	Not Archived	Not Archived	Not Archived	Not Archived	Not Archived	Not Archived	Not Archived	Not Archived

The CDP2 and FCDP measures forward laser light scattering and retrieve particle size assuming spherical liquid water droplet using Mie scattering theory. Given this theory, the relationship between scattering cross section measured by the instrument and the particle size is non monotonic. This can lead to oscillation within the measured particle size distribution (PSD) which can lead to misinterpretation of the shape of the PSD. In order to correct this phenomenon, we provide a reconstructed PSD based on Febvre (ICCP, 2016).

5.1.2 Quality assurance and quality control

5.1.2.1 CDP

Two CDP2 (first from Safire group and second from LaMP group) were used during the campaign as one broke due to overheating. No CDP was on the aircraft during four flights (as illustrated in Table 5.1). Both CDP were fully calibrated with water droplets (size and sampling area, Lance et al. 2011) and its optics aligned before the campaign. Several calibration were made using glass beads on site. This calibration has shown that the CDP was close to nominal and the actual integrating angles were 3.72-11.77° instead of the 4-12° given by the manufacturer. This 0.3° difference can lead to small difference in the PSD has seen in the comparison with the FCDP. The CDP2 optical system and data acquisition is similar to the others CDP on Twin Otter and Falcon 20. Besides, its position on the aircraft (alone on a POD under a wing), its extensive calibration, the extra care taken with cleaning the windows after or before each flights makes it the most suitable probe for providing the cloud droplet size distributions sampled by ATR42. Unfortunately, as it was not available four flights, the gap is filled with the FCDP which was located closed to the CDP2 and presented as follows.

5.1.2.2 FCDP

The FCDP was fully calibrated with water droplets (size and sampling area, Lance et al. 2011) and its optics aligned before the campaign. Calibrations were made using glass beads on site. An inter-comparaison with the CDP is shown on the Table 5.2. It can be seen that there is a good correlation either with the data acquired (PADS) or the reconstructed PSD (Monte Carlo). It should be noted that difference between FCDP and CDP can be accounted to the difference in size bins number which tends to make the PSD broader on the FCDP

Table 5-2 Total Concentration, Effective Diameter and Extinction coefficient ratio of FCDP over CDP2 with corresponding determination coefficient. Comparison made on 5 seconds averaged data with LWC larger than 10 mg/m3. Only flights with acceptable (yellow) or good (green) statistical sampling are reported. Monte-Carlo reconstruction done using Mie theory and integrating angles of 3.72 to 11.77° (MC 3.72-11.77) and integrating angles of 4 to 12° (MC 4-12).

Prob Corr.	#	CDP2 PADS – FCDP Dp>5µm						CDP2 MC (3.72-11.77) – FCDP Dp>5µm						CDP2 MC (4-12) – FCDP Dp>5µm					
Flight #		Total Conc.		Def f		Ext inct on		Total Conc.		Def f		Ext inct on		Total Conc.		Def f		Ext inct on	
		Slope	R^2	Slope	R^2	Slope	R^2	Slope	R^2	Slope	R^2	Slope	R^2	Slope	R^2	Slope	R^2	Slope	R^2
17	60	0.947	0.76	0.89	0.9	0.591	0.8	1.086	0.59	0.907	0.95	0.712	0.76	1.027	0.68	0.913	0.94	0.688	0.79
18	18	0.988	0.9	0.919	0.88	0.778	0.85	1.045	0.89	0.96	0.9	0.918	0.85	1.019	0.89	0.949	0.9	0.883	0.85
19	27	1.05	0.87	0.929	0.9	0.849	0.91	1.137	0.81	0.955	0.74	0.981	0.89	1.097	0.85	0.948	0.85	0.935	0.89
20	54	0.92	0.7	0.929	0.98	0.757	0.66	0.995	0.56	0.966	0.97	0.916	0.65	0.965	0.64	0.966	0.98	0.876	0.68
22	234	0.952	0.8	0.961	0.96	0.823	0.83	1.041	0.68	0.99	0.93	0.975	0.82	1.004	0.74	0.988	0.94	0.931	0.82
27	199	1.073	0.76	0.897	0.93	0.822	0.69	1.188	0.67	0.935	0.93	0.984	0.69	1.138	0.72	0.928	0.95	0.942	0.7
29	142	0.88	0.79	0.893	0.97	0.637	0.79	0.932	0.76	0.934	0.98	0.738	0.79	0.909	0.78	0.927	0.98	0.716	0.8
30	656	0.82	0.63	0.956	0.94	0.674	0.62	0.874	0.57	0.992	0.93	0.778	0.61	0.85	0.6	0.983	0.93	0.745	0.62
35	328	0.78	0.68	0.89	0.92	0.546	0.68	0.843	0.63	0.928	0.93	0.647	0.67	0.815	0.66	0.924	0.93	0.623	0.68
36	91	0.793	0.69	0.89	0.92	0.536	0.49	0.869	0.61	0.924	0.92	0.617	0.47	0.837	0.65	0.916	0.92	0.588	0.47
MOY		0.92	0.758	0.915		0.701		1.001		0.949		0.827		0.966	0.721	0.944	0.932	0.793	0.73
STD		0.102		0.028		0.12		0.119		0.028		0.144		0.111	0.095	0.027	0.038	0.136	0.126

5.1.2.3 D-S

The 2D-S was calibrated using a spinning disk with known size spots in laboratory and inter-compared with other 2D-S prior to the campaign at SPECinc factory. The 2D-S used a hermetic canister filled with nitrogen. No change in pressure was noticed in the canister which implied no need to refill it with “fresh” nitrogen.

5.2 F20

5.2.1 Instrumentation product and data availability

The cloud microphysics instrument package aboard Falcon includes a cloud and aerosol spectrometer with polarization CAS-DPOL (DMT, Baumgardner et al. 2011), and the 2D-stereo particle imager 2D-S (SPECinc; Lawson et al. 2006). The CAS-DPOL (30 size bins) samples cloud particle size range from 0.51 to 50 µm. Cloud particles in the size range from 10 to 1280 µm are imaged at 10 µm resolution and the size distribution is recorded with the 2D-S.

Table 5-3 Data status of the individual cloud instruments on board the Falcon 20 during DACCIWA.

Date 2016 day/month	29/JUNE	30/JUNE	01/JULY	05/JULY	06/JULY	07/JULY	08/JULY	10/JULY	11/JULY	12/JULY	13/JULY	14/JULY
take off (hhmmss)	131134	112032	111328	112502	094416	110152	083429	110642	103004	083118	091822	085602
take off (hhmmss)	152034	145201	142907	145720	131237	133457	120922	143846	141423	121828	124307	123339
Flight #	Flight 8	Flight 9	Flight 10	Flight 13	Flight 14	Flight 15	Flight 16	Flight 17	Flight 18	Flight 19	Flight 20	Flight 21
CMET data	archived	archived	archived	archived	archived	archived	archived	archived	archived	archived	archived	archived
CAS (0.5-50 µm)	archived	archived	archived	archived	archived	archived	archived	archived	archived	archived	archived	archived
2DS (10-1280µm)	archived	archived	archived	archived	archived	archived	archived	archived	archived	archived	archived	archived
Routing	Lomé-Save-Lomé	Lomé-Accra-Takoradi-Kumasi-Lomé	Lomé-Accra-Kumasi-Lomé	Lomé-Save-Lomé	Lomé-Abidjan-Lomé	Lomé-Accra-Lomé	Lomé-Lomé	Lomé-Takoradi-Jubilee-Lomé	Lomé-Abidjan-Espoir-Lomé	Lomé-Lomé	Lomé-Lomé	Lomé-Accra-Jubilee-Lomé

5.2.1.1 CAS-DPOL Cloud and Aerosol Spectrometer with Polarization

The CAS-DPOL measures particle size distributions between 0.51 and 50 µm at 1 Hz time resolution (Baumgardner et al., 2001). Its measurement principle is developed based on the FSSP-300 (Baumgardner et al., 1985). The intensity of forward scattered light in the angular range of 4 – 12° is detected and sorted into 30 size bins. Assuming Mie scattering theory, additional binning into 18 size bins is employed to rule out Mie ambiguities. Polarized backward scattered light is detected to investigate the sphericity and phase of the particles (Baumgardner et al., 2005; Gayet et al., 2012; Braga et al., 2017). Number concentrations are derived using the probe air speed measured by the probe.

5.2.1.2 2-Dimensional Stereo Probe 2D-S

The two-dimensional stereo (2D-S) probe (Lawson et al., 2006) detects the size and concentration of cloud droplets and ice particles in the size range of 10 to 1280 µm using shadow images of the cloud particles. Two orthogonal diode laser beams illuminate two linear diode arrays consisting of 128 photodiodes with 10 µm pixel resolution. When a particle crosses the laser beam in the sampling volume, its shadow image on the photodiode array is recorded by high-speed electronics. The diode lasers operate at 45 W and are single-mode and temperature-stabilized. This design with two lasers better defines the sampling volume boundaries and thus minimizes errors associated with the depths of field and the sizing of small particles. However, as the temperatures in the African lower troposphere were high during DACCIWA, the instrument had to be switched of several times particularly in cloud-free periods to avoid overheating.

5.2.2 Quality assurance and quality control

5.2.2.1 CAS-DPOL

The sampling area (SA) which is used to derive the number concentration of particles was characterized by a high-resolution scan with a droplet generator. 250 water droplets of a known, quasi constant size of about 40 µm were injected at and around the sensitive region perpendicular to the laser beam. The resolution of the droplet generator scan was 25 µm perpendicular to the laser beam and 50 µm along the laser beam. According to the scan, the area of the measured SA for particle diameters above 3 µm was 0.27 mm2, which is 8% higher than the initially reported SA by the manufacturer. Additionally, we estimate an uncertainty of the particle velocity in the CAS sampling tube of 15%, taking into account that particle velocities in the sampling tube may be slowed down or accelerated compared to open path instruments or the Pitot tube velocities at the CAS. This results in a combined uncertainty of the number concentration of ~21%.

A coincidence correction has been applied to the CAS data. As the Lance et al. (2012) correction did not fit to our CAS-DPOL, a CAS-DPOL intercomparison campaign with the DLR F20 in February 2017 was used to derive coincidence. During this campaign, 2 CAS-POL instruments were flown in parallel on the Falcon, with different slit configurations (0.8mm and 0.5mm) before the qualifying detector and identical configurations otherwise. While the instrument with the large orifice encountered significant coincidence, the instrument with the smaller orifice measured particle concentrations up to 2000 cm-3 without any significant coincidence effects as also derived from in the particle interarrival times. From this intercomparison, a coincidence correction was derived for the CAS-DPOL used during DACCIWA and applied to the data set. Thus for particle concentration significantly increasing the uncertainty for larger particle concentrations.
Calibrations with glass beads of four different sizes (2, 5, 20 and 42 µm) were performed between the flights to monitor the stability of the size bin classification. The size calibration was stable over the whole campaign. After the campaign a complete characterization of the CAS-DPOL was performed as suggested by Rosenberg et al. (2012) using in addition to borosilicate beads particles of different refractive indices (other gas types, latex, …). We estimate an uncertainty in particle size for particles diameters above 40 um on the order of 14 % and less below. The instrument had been installed previously on research aircraft during the ML-CIRRUS (Voigt et al., 2017) and ACCESS-II (Moore et al., 2017) campaigns.

5.2.2.2 2D-S

The 2D-S data processing is described in detail in the SPEC manual based on Korolov et al. (2007). We use SPEC method M4 for liquid spherical particles. M4 (All In, Ring-Spot Adjusted Spheres, length scale parallel to array and scaled based on white space) is appropriate in liquid water clouds or clouds with only quasi-spherical ice.). When the particle is considered in-focus due to < 10% white pixels for that image, the size is not corrected. In that case, the actual number of black pixels (the “projected area”) is used for the particle area unless $\pi(L1)^2/4$ < the projected area. This criterion forces the reported area for that particle to be less than or equal to that of a sphere with the same L1 (maximum length perpendicular to TAS direction) characteristic dimension. It may be a more appropriate criterion for liquid clouds, where L1 is typically the same as the maximum particle dimension. An algorithm was designed for correcting the size of spherical particles that are out-of-focus. Particles with dimension L1 < 365 µm and the particle image including > 10% white pixels, are assumed to be out-of-focus and the size of the particles is corrected according to the ratio of white and black areas (Korolev, 2007). The particle size after correction (L2) and the particles cross sectional area is computed as $\pi(L2)^2/4$.

An intercomparison of two different data evaluation methods for the same 2D-S data set from the Twin Otter flight 06 (SPEC M4 method and the Manchester Center-in Mean, and Manchester All-in Area equivalent) shows a reasonable agreement of the cloud droplet concentrations. Also, the comparison to CDP concentrations for particles >7.5 µm is reasonable.

Except for the smallest sizes, also the size distributions agree reasonably for the different data evaluation methods within the observed cloud sequence.

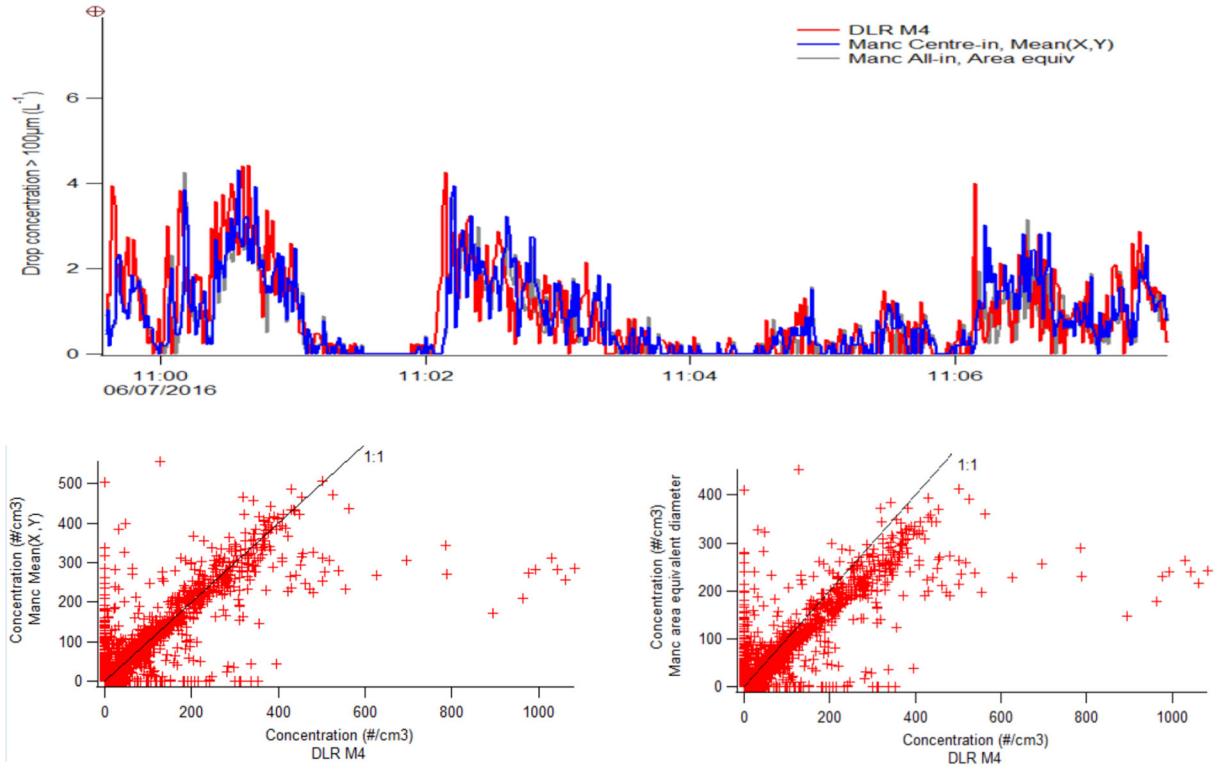

Figure 5-1 Upper panel: Cloud drop concentrations evaluated with the SPEC M4 data method and the Manchester Center in and all in data retrievals show a sufficient agreement. Lower panels: Scatterplot of the cloud drop concentrations evaluated with SPEC M4 and Manchester center-in and all-in.

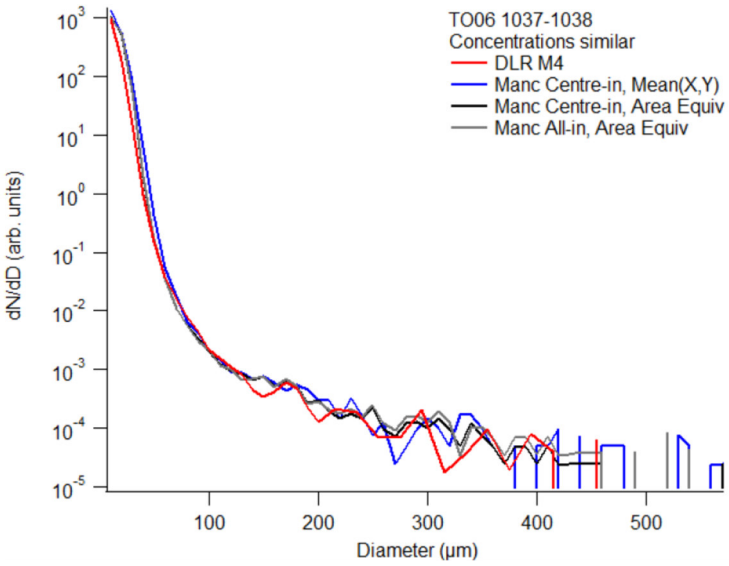

Figure 5-2 Particle size distribution of Twin Otter 2D-S data evaluated with the SPEC M4 data method and the Manchester Center-in Mean, and Center-in Area equivalent and All-in Area equiv data retrievals show a reasonable agreement for sizes > 50 µm.

5.3 TO

5.3.1 Instrumentation product and data availability

5.3.1.1 2DS

The 2DS is an optical array probe with a resolution of 10 µm. This is the same type of instrument as described in Section 5.1.1

5.3.1.2 CIP25

The CIP25 is an optical array probe with a resolution of 25 µm. See the next section for a comparison between the 2DS and CIP25.

5.3.1.3 CAS

The CAS measures both aerosol and cloud and is fully described in section 5.2.1.1 and 5.2.2.1. See these sections for details.

5.3.1.4 CDP

The CDP measures cloud droplets in the size range 2-50 µm. Its open path design means that it measures them in approximately ambient conditions. It was mounted under the nose of the Twin Otter. This instrument covers part of the size distribution range covered by the CAS, however the CDP is anecdotally regarded as a more reliable instrument as it uses only one gain stage and often its data is used ahead of the CAS where available. This particular instrument has had the "pinhole modification" described in Lance et al (2010). The pinhole modification screens out light scattered by particles close to the sample area (known as the unqualified area). This light can confuse the instrument and cause signals to be rejected as outside the sample area. The impact of this is that droplet concentrations saturate faster than would be expected from standard coincidence. See Lance et al (2010) for details.

Date	01-Jul	03-Jul	04-Jul	05-Jul	05-Jul	06-Jul	06-Jul	07-Jul	08-Jul	08-Jul	10-Jul	10-Jul	11-Jul	11-Jul	13-Jul	14-Jul	15-Jul	15-Jul
TAKE-OFF TIME	1410	1101	1155	1124	1600	0942	1355	0946	0836	1330	0854	1418	0817	1215	0859	0655	0930	1340
LANDING TIME	1725	1400	1515	1245	1750	1140	1637	1241	1127	1635	1133	1615	1024	1445	1205	0925	1205	1645
Instrument/ Property	TO01	TO02	TO03	TO04	TO05	TO06	TO07	TO08	TO09	TO10	TO11	TO12	TO13	TO14	TO15	TO16	TO17	TO18
CDP	Archived	Archived	Archived	Archived	Archived	Archived	Archived	Archived	Archived	Archived	Archived	Archived	Archived	Archived	Archived	Archived	Archived	Archived
CASPOL (CAPS)	Not archived	Not archived	Not archived	Not archived	Not archived	Not archived	Not archived	Not archived	Not archived	Not archived	Not archived	Not archived	Not archived	Not archived	Not archived	Not archived	Not archived	Not archived
CIP25 (CAPS)	Archived	Archived	Archived	Archived	Archived	Archived	Archived	Archived	Archived	Archived	Archived	Archived	Archived	Archived	Archived	Archived	Archived	Archived
Hotwire LWC (CAPS)	No data	No data	No data	No data	No data	No data	No data	No data	No data	No data	No data	No data	No data	No data	No data	No data	No data	No data
2DS	Archived	Archived	No data	Archived	No data	Archived	No data	No data	No data	No data	No data	No data	No data	No data	No data	No data	No data	No data

Table 5-4 Archived cloud data

The CDP and CAS performed well throughout the campaign and the data coverage was excellent. The 2DS was only installed for flights TO01 – TO04 and TO06, and was swapped for the PCASP for the other flights. The data coverage for these flights was 100%, except for TO03 where the data file was corrupted. The CAPS hotwire probe was operated on some flights, but the quality of the data was considered very poor. The baseline drift was in most cases larger than the real variation in the data. The data have therefore not been submitted to the data archive.

The archived cloud data are reported as the concentration in each size bin at ambient temperature and pressure on a 1 s timescale. The CDP data file also includes calculated values for total CDNC, MVD, LWC, effective radius, and mean diameter.

5.3.2 Quality assurance and quality control

5.3.2.1 CDP & CAS

The CAS was calibrated once during the campaign on 29th Jun 2016 using PSL and borosilicate glass microspheres. Like the PCASP the instrument uses three gain stages to cover its full size range. Because its minimum diameter is larger than that of the PCASP sufficient samples were available to calibrate all gain stages. Again, the Rosenberg (2012) method was used. This method allows the user to correct the calibration for the effects of sample refractive index. The CDP also was calibrated once during the field project on the 29th June 2016 using borosilicate glass microspheres and the Rosenberg (2012) method. Contact Phil Rosenberg or Jonathan Taylor for details and software. Figure 5.2 shows good overall correlation between the CAS and CDP CDNC and LWC in the size range overlap. However, there is some evidence that at higher concentrations the CAS undercounts compared to the CDP, and this issue was seen in flights with high CDNC, which suggests the CAS was undercounting due to coincidence (Lance et al., 2012). For this reason, only the CDP data have been archived as they are considered of a higher quality than the Twin Otter CAS data.

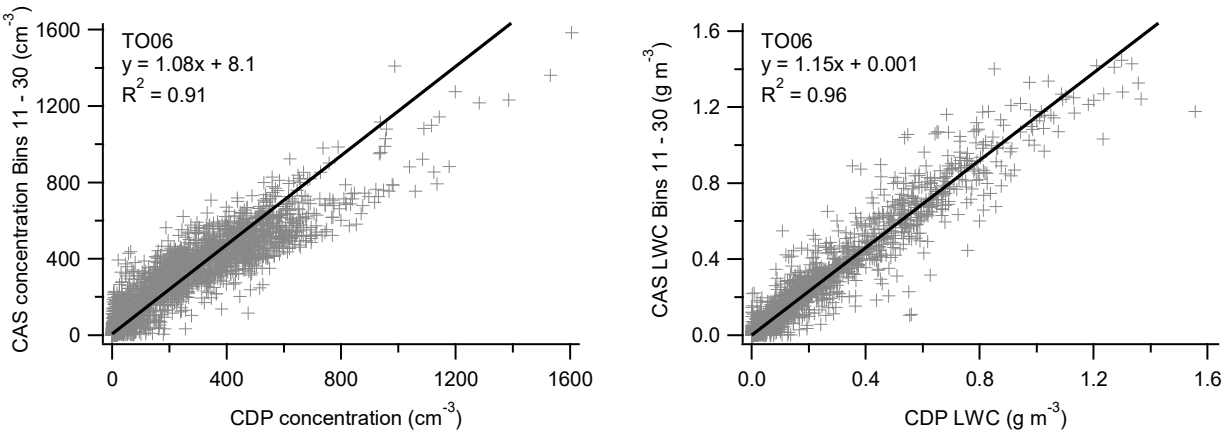

Figure 5-3 Comparison of CDNC and LWC measured by the CAS and CDP on the Twin Otter from flight TO06.

5.3.2.2 2DS

The 2DS instrument does not require size calibration before each flight as the resolution and sample area are fixed. Detailed checks were carried out in the lab before and after the experiment and no problems were found. The Twin Otter 2DS data were processed using optical array shadow imaging software (OASIS) v1.4991. The software processing was the same as described by Taylor et al. (2016), though shape analysis was not performed as all the measurements were carried out below the freezing level. Particles with inter-arrival times $<10^{-6}$ s were removed as shattering artefacts and an overload correction was applied for occasional periods where the probe's databanks were overloaded. Particles over 10 pixels long and 1 pixel wide were discounted as 'streaking' artefacts due to stuck pixels. The sample volume was calculated using the centre-in method and the measured true airspeed, and particle sizes were calculated using the mean(X,Y) diameter, and out-of focus particles were corrected using the method described by Korolev et al. (2007). Figure 5.3 shows a good correlation and similar concentrations for the 2DS and CDP concentrations for flight TO02 in the overlap size range. Readers should note, however, that the slope of this comparison is very sensitive to the choice of bins as the cloud drop size distribution is so steep in this size range, a small error in sizing causes a larger error in concentration. The sizing uncertainty in any 2DS is not well quantified. The first two size bins of the 2DS are not used in this comparison as these are often unreliable in OAP probes due to the limited resolution of the probe.

A software intercomparison exercise was carried out, which involved all three groups using a 2DS (UNIVMAN, DLR and LaMP) processing the same raw data file from flight TO06 using their respective software and settings. The derived total concentrations agreed within ±20%, and drizzle concentrations agreed within ±5%. This is a similar level of agreement as was found when comparing the concentrations using mean(X,Y) diameter and area-equivalent diameter using the UNIMAN OASIS code, and is within the approximate factor of two uncertainty associated with optical array probes.

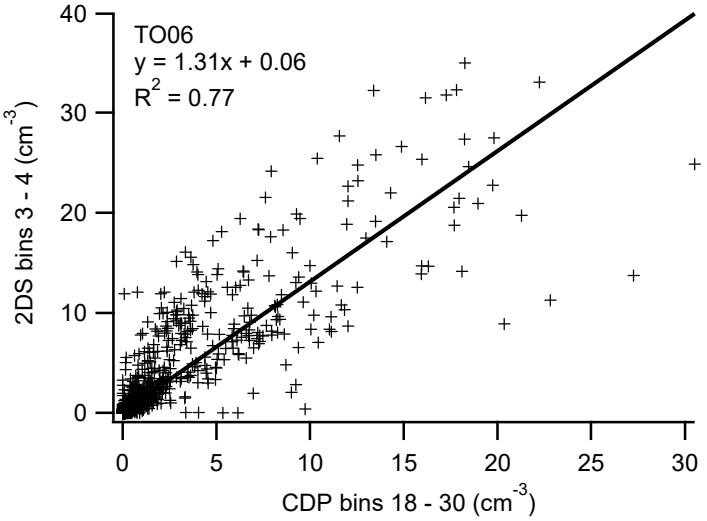

Figure 5-4 Comparison of Twin Otter 2DS and CDP concentrations over the overlapping size range of ~25 – 45 µm.

5.3.2.3 CIP25

The CIP25 was operated in the same way as the 2DS, and both the pre-flight checks and data processing were identical with the exception that the CIP25 does not provide the relevant diagnostics for an overload correction. Figure 5.3 shows a comparison of the drizzle concentrations measured by the CIP25 and 2DS, which showed a good correlation and agreement to around ±30%. As in Figure 5.3, this comparison is very sensitive to the choice of size bins due to the steep slope of the size distribution, and the sizing uncertainty is not well quantified.

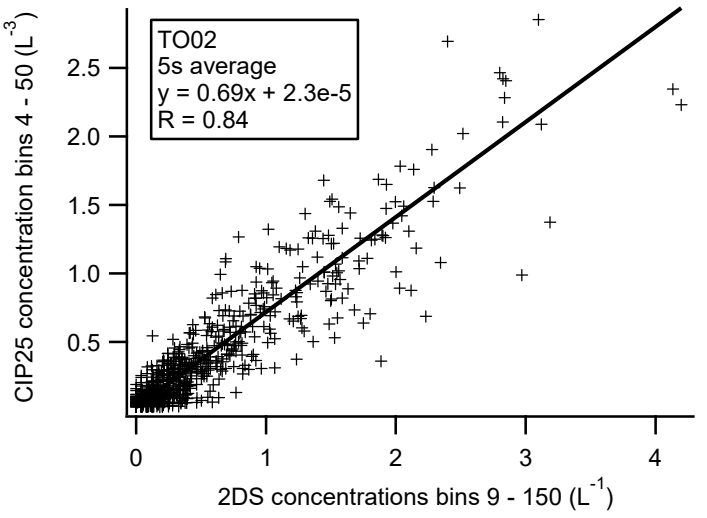

Figure 5-5 Comparison of Twin Otter CIP25 and 2DS drizzle concentrations in the size range ~100 – 1000 µm.

6 References

Bahreini, R. E.J. Dunlea, B.M. Matthew, C. Simons, K.S. Docherty, P.F. Carlo, J.L. Jimenez, C.A. Brock, A.M. Middlebrook (2008). "Design and operation of a pressure-controlled inlet for airborne sampling with an aerodynamic aerosol lens." Aerosol science and Technology., 42(6), doi:10.1080/02786820802178514

Baumgardner, D., Popovicheva, O., Allan, J., Bernardoni, V., Cao, J., Cavalli, F., Cozic, J., Diapouli, E., Eleftheriadis, K., Genberg, P. J., Gonzalez, C., Gysel, M., John, A., Kirchstetter, T. W., Kuhlbusch, T. A. J., Laborde, M., Lack, D., Müller, T., Niessner, R., Petzold, A., Piazzalunga, A., Putaud, J. P., Schwarz, J., Sheridan, P., Subramanian, R., Swietlicki, E., Valli, G., Vecchi, R., and Viana, M.: Soot reference materials for instrument calibration and intercomparisons: a workshop summary with recommendations, Atmos. Meas. Tech., 5, 1869-1887, 10.5194/amt-5-1869-2012, 2012.

Baumgardner, D., Strapp, W. and Dye, J. E.: Evaluation of the forward scattering spectrometer probe. Part II: corrections for coincidence and dead-time losses, J. Atmos. Ocean. Technol., 2(4), 626–632, 1985.

Baumgardner, D., Jonsson, H., Dawson, W., O'Connor, D. and Newton, R.: The cloud, aerosol and precipitation spectrometer: a new instrument for cloud investigations, Atmos. Res., 59-60, 251–264, doi:10.1016/S0169-8095(01)00119-3, 2001.

Baumgardner, D., Chepfer, H., Raga, G. B. and Kok, G. L.: The shapes of very small cirrus particles derived from in situ measurements, Geophys. Res. Lett., 32(1), 1–4, doi:10.1029/2004GL021300, 2005

Braga, R. C., Rosenfeld, D., Weigel, R., Jurkat, T., Andreae, M. O., Wendisch, M., Pöhlker, M. L., Klimach, T., Pöschl, U., Pöhlker, C., Voigt, C., Mahnke, C., Borrmann, S., Albrecht, R. I., Molleker, S., Vila, D. A., Machado, L. A. T., and Artaxo, P.: Comparing calculated microphysical properties of tropical convective clouds at cloud base with measurements during the ACRIDICON-CHUVA campaign, Atmos. Chem. Phys. Discuss., doi:10.5194/acp-2016-872, 2017.

Bohren, C. F., and Huffman, D. R.: Absorption and scattering of light by small particles, Wiley, New York, 1983.

Bond, T. C., Anderson, T. L. and Campbell, D.: Calibration and Intercomparison of Filter-Based Measurements of Visible Light Absorption by Aerosols, Aerosol Sci. Technol., 30(6), 582–600, doi:10.1080/027868299304435, 1999

Crumeyrolle, S.; Gomes, L.; Tulet, P.; Matsuki, A.; Schwarzenboeck, A.; Crahan, K. 2008: Increase of the aerosol hygroscopicity by cloud processing in a mesoscale convective system: a case study from the AMMA campaign. Atmos. Chem. Phys. Vol. 8, No. 23, p. 6907-6924. SRef-ID 1680-7324/acp/2008-8-6907 (EGU)

Drewnick, F., Highs, S. S., DeCarlo, P. Jayne, J. T., Gonin, M., Fuhrer, K., Weimer, S., Jimenez, J. L., Demerjian, K. L., Borrmann, S. and Worsnopp, D. R.: A new Time-of-Flight Aerosol Mass Spectrometer (TOF-AMS) - instrument description and first field deployment, Aerosol Sci. Technol., 39(7), 637-658, doi: 10.1080/02786820500182040, 2007.

Febvre G., D. Leroy, V. Shcherbakov, and A. Schwarzenboeck. Improving the retrieval of particle size spectra and liquid water content from optical spectrometer measurements using a Monte Carlo inversion method. 17th ICCP (International Conference on Clouds and Precipitation), July 25-29, 2016.

Gayet, J.-F., V. Shcherbakov, C. Voigt, U. Schumann, D. Schäuble, P. Jessberger, A. Petzold, A. Minikin, H. Schlager, O. Dubovik, and T. Lapyonok: The evolution of microphysical and optical properties of an A380 contrail in the vortex phase, Atmos. Chem. Phys., 12, 6629-6643, doi:10.5194/acp-12-6629-2012, 2012.

Jeβberger, P., Voigt, C., Schumann, U., Sölch, I., Schlager, H., Kaufmann, S., Petzold, A., Schäuble, D. and Gayet, J. F.: Aircraft type influence on contrail properties, Atmos. Chem. Phys., 13(23), 11965–11984, doi:10.5194/acp-13-11965-2013, 2013.

Holden, N. E. and Lide, D. R.: CRC handbook of chemistry and physics, 1991.

Korolev, A. and Korolev, A.: Reconstruction of the Sizes of Spherical Particles from Their Shadow Images. Part I: Theoretical Considerations, J. Atmos. Ocean. Technol., 24(3), 376–389, doi:10.1175/JTECH1980.1, 2007.

Korolev A. and B. Sussman, 2000: A Technique for Habit Classification of Cloud Particles, Journal of Atmospheric and Oceanic Technologies, 17, 8.

Kuwata, M., Zorn, S. R. and Martin, S. T.: Using elemental ratios to predict the density of organic material composed of carbon, hydrogen, and oxygen., Environ. Sci. Technol., 46(2), 787–94, doi:10.1021/es202525q, 2012.

Laborde, M., Mertes, P., Zieger, P., Dommen, J., Baltensperger, U., and Gysel, M.: Sensitivity of the Single Particle Soot Photometer to different black carbon types, Atmos. Meas. Tech., 5, 1031-1043, 10.5194/amt-5-1031-2012, 2012.

Laborde, M., Schnaiter, M., Linke, C., Saathoff, H., Naumann, K.-H., Möhler, O., Berlenz, S., Wagner, U., Taylor, J. W., Liu, D., Flynn, M., Allan, J. D., Coe, H., Heimerl, K., Dahlkötter, F., Weinzierl, B., Wollny, A. G., Zanatta, M., Cozic, J., Laj, P., Hitzenberger, R., Schwarz, J. P. and Gysel, M.: Single Particle Soot Photometer intercomparison at the AIDA chamber, Atmos. Meas. Tech., 5(12), 3077–3097, doi:10.5194/amt-5-3077-2012, 2012.

Lance, S.: Coincidence Errors in a Cloud Droplet Probe (CDP) and a Cloud and Aerosol Spectrometer (CAS), and the Improved Performance of a Modified CDP, J. Atmos. Ocean. Technol., 29(10), 1532–1541, doi:10.1175/JTECH-D-11-00208.1, 2012.

Lawson, R. and B. Baker, 2006: Improvement in Determination of Ice Water Content from Two Dimensional Particle Imagery. Part II: Applications to Collected Data. J. Appl. Meteor. Climatol., 45, 1291–1303, doi: 10.1175/JAM2399.1.

Lawson, R. P., O'Connor, D., Zmarzly, P., Weaver, K., Baker, B. A., Mo, Q., and Jonsson, H.: The 2D-S (Stereo) probe: design and preliminary tests of a new airborne, high speed, high-resolution particle imaging probe, J. Atmos. Oceanic Technol., 23, 1462–1477, 2006.

Lance, S.: Coincidence errors in a cloud droplet probe (CDP) and a cloud and aerosol spectrometer (CAS), and the improved performance of a modified CDP, J. Atmos. Ocean. Technol., 29(10), 1532–1541, doi:10.1175/JTECH-D-11-00208.1, 2012.

Mallaun, C., Giez, A. and Baumann, R.: Calibration of 3-D wind measurements on a single-engine research aircraft, Atmos. Meas. Tech., 8(8), 3177–3196, doi:10.5194/amt-8-3177-2015, 2015.

Massoli, P. Kebabian, P. L., Onasch, T. B., Hills, F. B. and Freedman, A.: Aerosol light extinction measurements by Cavity Attenuated Phase Shift (CAPS) spectroscopy: laboratory validatio n and field deployment of a compact aerosol particle extinction monitor. Aerosol Sci. Technol., 44, 428-435, 2009

Moore, R. H., Thornhill, K. L., Weinzierl, B., Sauer, D., D'Ascoli, E., Kim, J., Lichtenstern, M., Scheibe, M., Beaton, B., Beyersdorf, A. J., Barrick, J., Bulzan, D., Corr, C. A., Crosbie, E., Jurkat, T., Martin, R., Riddick, D., Shook, M., Slover, G., Voigt, C., White, R., Winstead, E., Yasky, R., Ziemba, L. D., Brown, A., Schlager, H., and Anderson, B. E.: Biofuel blending reduces particle emissions from aircraft engines at cruise conditions, Nature, 543, 411-415, 10.1038/nature21420, 2017.

Liu, Y. G., and Daum, P. H.: Relationship of refractive index to mass density and self-consistency of mixing rules for multicomponent mixtures like ambient aerosols, Journal of Aerosol Science, 39, 974-986, 10.1016/j.jaerosci.2008.06.006, 2008.

Massoli, P., Kebabian, P. L., Onasch, T. B., Hills, F. B., and Freedman, A., Aerosol light extinction measurements by Cavity Attenuated Phase Shift (CAPS) Spectroscopy: Laboratory validation and field deployment of a compact aerosol particle extinction monitor, Aerosol Sci. Tech., 44, 428–435, doi:10.1080/02786821003716599, 2010.

Middlebrook, A. M., Bahreini, R., Jimenez, J. L. and Canagaratna, M. R.: Evaluation of Composition-Dependent Collection Efficiencies for the Aerodyne Aerosol Mass Spectrometer using Field Data, Aerosol Sci. Technol., 46(3), 258–271, doi:10.1080/02786826.2011.620041, 2012.

Nobuhiro Moteki & Yutaka Kondo (2010) Dependence of LaserInduced Incandescence on Physical Properties of Black Carbon Aerosols: Measurements and Theoretical Interpretation, Aerosol Science and Technology, 44:8, 663-675, DOI: 10.1080/02786826.2010.484450.

Müller, T., Henzing, J. S., de Leeuw, G., Wiedensohler, A., Alastuey, A., Angelov, H., Bizjak, M., Collaud Coen, M., Engström, J. E., Gruening, C., Hillamo, R., Hoffer, A., Imre, K., Ivanow, P., Jennings, G., Sun, J. Y., Kalivitis, N., Karlsson, H., Komppula, M., Laj, P., Li, S.-M., Lunder, C., Marinoni, A., Martins dos Santos, S., Moerman, M., Nowak, A., Ogren, J. A., Petzold, A., Pichon, J. M., Rodriquez, S., Sharma, S., Sheridan, P. J., Teinilä, K., Tuch, T., Viana, M., Virkkula, A., Weingartner, E., Wilhelm, R. and Wang, Y. Q.: Characterization and intercomparison of aerosol absorption photometers: result of two intercomparison workshops, Atmos. Meas. Tech., 4(2), 245–268, doi:10.5194/amt-4-245-2011, 2011a.

Müller, T., Laborde, M., Kassell, G. and Wiedensohler, A.: Design and performance of a three-wavelength LED-based total scatter and backscatter integrating nephelometer, Atmos. Meas. Tech., 4(6), 1291–1303, doi:10.5194/amt-4-1291-2011, 2011b.

Park, K., Kittelson, D. B., Zachariah, M. R. and Mcmurry, P. H.: Measurement of inherent material density of nanoparticle agglomerates, J. Nanoparticle Res., 6, 267–272, doi:10.1023/B:NANO.0000034657.71309.e6, 2004.

Rosenberg, P. D., Dean, A. R., Williams, P. I., Dorsey, J. R., Minikin, A., Pickering, M. A. and Petzold, A.: Particle sizing calibration with refractive index correction for light scattering optical particle counters and impacts upon PCASP and CDP data collected during the Fennec campaign, Atmos. Meas. Tech., 5(5), 1147–1163, doi:10.5194/amt-5-1147-2012, 2012.

Sellegri K., P. Laj, R. Dupuy, J.P. Putaud. Size-dependent scavenging efficiencies of multicomponent atmospheric aerosols in clouds. JGR 108(D11), 2003

Snider J.R. and J.L. Brenguier. Cloud condensation nuclei and cloud droplet measurements during ACE-2. Tellus. 2000, 52B, 828-842.

Taylor, J. W., Choularton, T. W., Blyth, A. M., Liu, Z., Bower, K. N., Crosier, J., Gallagher, M. W., Williams, P. I., Dorsey, J. R., Flynn, M. J., Bennett, L. J., Huang, Y., French, J., Korolev, A. and Brown, P. R. A.: Observations of cloud microphysics and ice formation during COPE, Atmos. Chem. Phys., 16(2), 799–826, doi:10.5194/acp-16-799-2016, 2016.

Villani, P.; Picard, D.; Marchand, N.; Laj, P. 2007. Design and Validation of a 6-Volatility Tandem Differential Mobility Analyzer (VTDMA). Aerosol Sci. Technol. Vol. 41, No. 10 , p. 898-906 DOI 10.1080/02786820701534593 .

Voigt, C., Schumann, U., Minikin, A., Abdelmonem, A., Afchine, A., Borrmann, S., Boettcher, M., Buchholz, B., Bugliaro, L., Costa, A., Curtius, J., Dollner, M., Dörnbrack, A., Dreiling, V., Ebert, V., Ehrlich, A., Fix, A., Forster, L., Frank, F., Fütterer, D., Giez, A., Graf, K., Grooß, J., Groß, S., Heimerl, K., Heinold, B., Hüneke, T., Järvinen, E., Jurkat, T., Kaufmann, S., Kenntner, M., Klingebiel, M., Klimach, T., Kohl, R., Krämer, M., Krisna, T., Luebke, A., Mayer, B., Mertes, S., Molleker, S., Petzold, A., Pfeilsticker, K., Port, M., Rapp, M., Reutter, P., Rolf, C., Rose, D., Sauer, D., Schäfler, A., Schlage, R., Schnaiter, M., Schneider, J., Spelten, N., Spichtinger, P., Stock, P., Walser, A., Weigel, R., Weinzierl, B., Wendisch, M., Werner, F., Wernli, H., Wirth, M., Zahn, A., Ziereis, H. and Zöger, M.: ML-CIRRUS - the airborne experiment on natural cirrus and contrail cirrus with the high-altitude long-range research aircraft HALO, Bull. Am. Meteorol. Soc., doi:10.1175/BAMS-D-15-00213.1, 2016.

Weigel, R., Spichtinger, P., Mahnke, C., Klingebiel, M., Afchine, A., Petzold, A., Krämer, M., Costa, A., Molleker, S., Jurkat, T., Minikin, A. and Borrmann, S.: Thermodynamic correction of particle concentrations measured by underwing probes on fast flying aircraft, Atmos. Meas. Tech., 9, 5135-5162 , doi:10.5194/amt-9-5135, 2016.